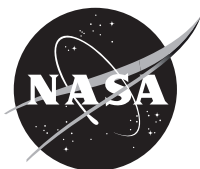


NASA/TM–2012-104606 / Vol 29



**Technical Report Series on Global Modeling and Data Assimilation,
Volume 29**

Max J. Suarez, Editor

**Atmospheric Reanalyses—Recent Progress and Prospects
for the Future.**

A Report from a Technical Workshop, April 2010

*Michele M. Rienecker, Dick Dee, Jack Woollen, Gilbert P. Compo, Kazutoshi Onogi, Ron Gelaro,
Michael G. Bosilovich, Arlindo da Silva, Steven Pawson, Siegfried Schubert, Max Suarez, Dale Barker,
Hirotaka Kamahori, Robert Kistler, and Suranjana Saha*

National Aeronautics and
Space Administration

**Goddard Space Flight Center
Greenbelt, Maryland 20771**

June 2012

NASA STI Program ... in Profile

Since its founding, NASA has been dedicated to the advancement of aeronautics and space science. The NASA scientific and technical information (STI) program plays a key part in helping NASA maintain this important role.

The NASA STI program operates under the auspices of the Agency Chief Information Officer. It collects, organizes, provides for archiving, and disseminates NASA's STI. The NASA STI program provides access to the NASA Aeronautics and Space Database and its public interface, the NASA Technical Report Server, thus providing one of the largest collections of aeronautical and space science STI in the world. Results are published in both non-NASA channels and by NASA in the NASA STI Report Series, which includes the following report types:

- **TECHNICAL PUBLICATION.** Reports of completed research or a major significant phase of research that present the results of NASA Programs and include extensive data or theoretical analysis. Includes compilations of significant scientific and technical data and information deemed to be of continuing reference value. NASA counterpart of peer-reviewed formal professional papers but has less stringent limitations on manuscript length and extent of graphic presentations.
- **TECHNICAL MEMORANDUM.** Scientific and technical findings that are preliminary or of specialized interest, e.g., quick release reports, working papers, and bibliographies that contain minimal annotation. Does not contain extensive analysis.
- **CONTRACTOR REPORT.** Scientific and technical findings by NASA-sponsored contractors and grantees.
- **CONFERENCE PUBLICATION.** Collected papers from scientific and technical conferences, symposia, seminars, or other meetings sponsored or co-sponsored by NASA.
- **SPECIAL PUBLICATION.** Scientific, technical, or historical information from NASA programs, projects, and missions, often concerned with subjects having substantial public interest.
- **TECHNICAL TRANSLATION.** English-language translations of foreign scientific and technical material pertinent to NASA's mission.

Specialized services also include organizing and publishing research results, distributing specialized research announcements and feeds, providing help desk and personal search support, and enabling data exchange services. For more information about the NASA STI program, see the following:

- Access the NASA STI program home page at <http://www.sti.nasa.gov>
 - E-mail your question via the Internet to help@sti.nasa.gov
 - Fax your question to the NASA STI Help Desk at 443-757-5803
 - Phone the NASA STI Help Desk at 443-757-5802
 - Write to:
NASA STI Help Desk
NASA Center for AeroSpace Information
7115 Standard Drive
Hanover, MD 21076-1320
-



**Technical Report Series on Global Modeling and Data Assimilation,
Volume 29**

Max J. Suarez, Editor

**Atmospheric Reanalyses—Recent Progress and Prospects
for the Future.**

A Report from a Technical Workshop, April 2010

*Michele M. Rienecker
Goddard Space Flight Center, Greenbelt, Maryland*

*Dick Dee
European Centre for Medium-Range Weather
Forecasts, Reading, United Kingdom*

*Jack Woollen
I.M. Systems Group, Inc., Rockville, Maryland*

*Gilbert P. Compo
University of Colorado, Boulder, Colorado*

*Kazutoshi Onogi
Japan Meteorological Agency, Tokyo, Japan*

*Ron Gelaro
Goddard Space Flight Center, Greenbelt, Maryland*

*Michael G. Bosilovich
Goddard Space Flight Center, Greenbelt, Maryland*

*Arlindo da Silva
Goddard Space Flight Center, Greenbelt, Maryland*

*Steven Pawson
Goddard Space Flight Center, Greenbelt, Maryland*

*Siegfried Schubert
Goddard Space Flight Center, Greenbelt, Maryland*

*Max Suarez
Goddard Space Flight Center, Greenbelt, Maryland*

*Dale Barker
Met Office, Exeter, United Kingdom*

*Hiroataka Kamahori
Meteorological Research Institute
Japan Meteorological Agency, Tsukuba, Japan*

*Robert Kistler
NOAA National Centers for Environmental Prediction
Camp Springs, Maryland*

*Suranjana Saha
NOAA National Centers for Environmental Prediction
Camp Springs, Maryland*

National Aeronautics and
Space Administration

**Goddard Space Flight Center
Greenbelt, Maryland 20771**

Notice for Copyrighted Information

This manuscript has been authored by employees of *the European Centre for Medium-Range Weather Forecasts, Reading, United Kingdom; I.M. Systems Group, Inc. in Rockville, Maryland; The University of Colorado; the Japan Meteorological Agency; Met Office, Exeter, United Kingdom; and the NOAA National Centers for Environmental Prediction* with the National Aeronautics and Space Administration. The United States Government has a non-exclusive, irrevocable, worldwide license to prepare derivative works, publish, or reproduce this manuscript, and allow others to do so, for United States Government purposes. Any publisher accepting this manuscript for publication acknowledges that the United States Government retains such a license in any published form of this manuscript. All other rights are retained by the copyright owner.

Trade names and trademarks are used in this report for identification only. Their usage does not constitute an official endorsement, either expressed or implied, by the National Aeronautics and Space Administration.

Level of Review: This material has been technically reviewed by technical management

Available from:
NASA Center for AeroSpace Information
7115 Standard Drive
Hanover, MD 21076-1320

National Technical Information Service
5285 Port Royal Road
Springfield, VA 22161 Price Code: A17

Abstract

In April 2010, developers representing each of the major reanalysis centers met at Goddard Space Flight Center to discuss technical issues – system advances and lessons learned – associated with recent and ongoing atmospheric reanalyses and plans for the future. The meeting included overviews of each center’s development efforts, a discussion of the issues in observations, models and data assimilation, and, finally, identification of priorities for future directions and potential areas of collaboration. This report summarizes the deliberations and recommendations from the meeting as well as some advances since the workshop.

Table of Contents

List of Figures	vi
1. Introduction.....	1
2. Major System Advances	1
2.1 Model	1
2.2 Analysis and Assimilation.....	2
2.3 Observations.....	4
3. Quality of the Reanalyses.....	4
3.1 Evaluations through weather forecast skill.....	5
3.2 Climate-related Diagnostics.....	7
3.2.1 <i>Water and Energy Cycles</i>	7
3.2.2 <i>Interannual Variability</i>	11
3.2.3 <i>Sub-seasonal and Higher Frequency Variability</i>	14
3.2.4 <i>The Stratosphere</i>	18
3.3 Trends and Long-term Variability	20
4. Planning Future Atmospheric Reanalyses.....	24
4.1 Model	25
4.2 Assimilation System	25
4.3 Observations.....	27
4.4 Anticipated Developments in Coupling to Other Components.....	31
4.4.1 <i>Upper ocean and land surface</i>	31
4.4.2 <i>Carbon, aerosols, other constituents</i>	31
5. Cross-Center Coordination for the Next-generation Reanalyses	31
5.1 Observations.....	32
5.2 Innovative Diagnostics.....	32
5.3 Standard Intercomparisons and Benchmarks Including Community Involvement.....	33
5.4 Coordinating Ancillary Products: Accessible Assimilated Observations and Statistics	33
5.5 Moving Forward	33
6. Summary of Recommendations	34
7. References	35
Appendix A: Summary of Recent and Ongoing Reanalyses	39
Appendix B: Summary of Reanalyses to Date	42
Appendix C: Acronyms.....	43
Appendix D: Acknowledgements	45

List of Figures

Figure 1: Tropical averages (20°S-20°N) of 12-hourly variational bias estimates (K) for HIRS channel 11 radiance data from NOAA-11 and NOAA-12 in ERA-Interim.....	3
Figure 2: Global mean 12-hourly variational bias estimates (K) for MSU channel 2 radiance data from NOAA-10, NOAA-11, NOAA-12, and NOAA-14. The upper panel is from ERA-Interim (from Dee and Uppala, 2009) and the lower panel is from MERRA. The latter uses MSU data from NOAA/NESDIS that has been intercalibrated using the simultaneous nadir overpass (SNO) method (Zou et al. 2006).....	3
Figure 3a: Extratropical anomaly correlations for 3-, 5-, and 7-day forecasts of 500 hPa height based on the ECMWF operational forecast system (top) and the ERA-Interim and ERA-40 reanalyses (bottom), after Dee and Uppala (2009).....	5
Figure 3b: Yearly averaged (left) Southern Hemisphere and (right) Northern Hemisphere 00 UTC 120-h forecast anomaly correlations for CFSR (black triangles), operational GFS (red circles), CFSR-Lite (green squares), CFS R2 (purple diamonds), and CDAS R1 (blue stars).....	6
Figure 4: (a) The time series of the spatial correlation of annual mean precipitation averaged over the tropics (15°S-15°N) from several reanalyses and CMAP (black curve) with that from GPCP. (b) The annual mean spatial standard deviation of precipitation (mm day ⁻¹) over the tropics. The black dashed line denotes GPCP.....	7
Figure 5a: The precipitation bias (mm day ⁻¹) in several reanalyses relative to GPCP, January 1990-2002..	7
Figure 5b: Taylor diagrams of annual mean precipitation from reanalyses using GPCP as a reference and CMAP as an additional observational reference. Each panel shows the statistics for different regions: (a) globe, (b) tropics, (c) global land, and (c) global oceans. The red and blue lines show limits of expected high and low correlation as determined by comparing GPCP and CMAP observations. See Bosilovich et al. (2008) for details.	8
Figure 6: MERRA's estimate of the vertically integrated water vapor budget for January 2004, in kg m ⁻² day ⁻¹	9
Figure 7: The joint frequency distribution of the top-of-atmosphere long-wave (abscissa) and short-wave (ordinate) fluxes for 2004 from MERRA, NCEP-DOE R2, and JRA-25. For comparison, the results are shown from CERES. The solid line contours from CERES overlay the shaded contours in all panels.....	9
Figure 8: The global energy budget (W m ⁻²). The numbers in black and white are those from satellite data climatologies and other observations for the period 2000-2005 from Trenberth et al. (2009). The colored values are from reanalyses for the 2002-2008 period (except ERA40): MERRA (red), NCEP-NCAR R1 (green), ERA40 (brown), CFSR (orange), JRA-25 (blue), NCEP-DOE R2 (purple), ERA-Interim (cyan), and 20CR (green).....	10
Figure 9: The lag correlation of precipitation and SST for winter over the Western Pacific. The correlation for CFSR is compared with that from observations, NCEP-NCAR R1, and NCEP-DOE R2. Positive lags denote precipitation is leading SST.....	11
Figure 10: The eddy height field at 300 hPa for January 1995 (upper row) and January 1998 (middle row) from MERRA (first column) and ERA-Interim (second column). The differences between MERRA and ERA-Interim are shown in the third column while the fourth column compares MERRA with ERA-40. The bottom panels show the differences between the two years.....	11

Figure 11: Correlations of MERRA with other estimates of selected monthly-mean quantities in January. The comparisons with ERA-Interim (300 hPa eddy height, vertical velocity at 500 hPa, u-wind at 850 hPa and specific humidity (q) at 850 hPa) are for 1990-2008. The comparison with SSM/I (TPW) is for 1993-2002, and the comparison with GPCP v2.1 (precipitation) is for 1979-2008.....12

Figure 12: Zonal mean values of the correlation between MERRA and ERA-Interim, and between MERRA and selected observational data sets, for various monthly-mean quantities during January (left-hand panels) and July (right-hand panels) for the period 1990 to 2008. Comparisons with GPCP precipitation and from NOAA’s OLR product are also included.....13

Figure 13: Time series of anomaly pattern correlations between monthly mean anomaly fields of northern hemisphere extratropical 300 hPa geopotential height from two upper-air based reanalyses and 20CR for the months of December (cool colors) and June (warm colors). Correlations with ERA-40 are shown by the blue and red curves. The black curves show the expected anomaly pattern correlations when only the observed SST fields are available for the months of (thick) December and (thin) June using the ECHAM4.5 atmospheric model forced with observed SSTs (courtesy of the International Research Institute). The thin black lines show the mean value of these expected correlations, with the thicker line corresponding to December and the thinner corresponding to June.....14

Figure 14: Wavenumber-frequency diagram for precipitation, following Wheeler and Kiladis (1999). ER is equatorial Rossby wave; EIG is eastward inertio-gravity wave, MRG is mixed Rossby-gravity wave. The calculations are based on daily precipitation for 1989-2008 averaged between 15°S and 15°N. For each product, the left-hand panel is the symmetric component and the right-hand panel is the anti-symmetric component.....15

Figure 15: Tropical cyclone detection rate from CFSR.....16

Figure 16: Maximum intensity of tropical storms in the Atlantic detected in MERRA over the period 1998-2005, compared with observations from 1997 to 2008.....16

Figure 17: Diurnal variation in precipitation (mm day⁻¹) over the United States for July 2004. The July mean has been removed. Results are shown as 6-hour averages for TRMM observations, and for the reanalyses: MERRA, ERA-Interim, CFSR, JRA-25, NCEP-DOE R2, and NCEP-NCAR R1.....17

Figure 18: Map of the local anomaly correlation between four-times daily anomalies of 300hPa geopotential from ERA-40 and 20CR for the period 1979 – 2001. The thick black line contour indicates the region where ERA-40 and NCEP-NCAR R1 correlate highly (0.975) in this quantity during this period.....18

Figure 19a: Time series of the monthly mean zonal velocity at Singapore from (top) rawinsonde observations, (center) NCEP-NCAR R1, and (bottom) ERA-15. The contour interval is 10 ms⁻¹, the 15 ms⁻¹ and 25 ms⁻¹ are also included (dashed) and positive values (i.e. westerlies) are shaded.....19

Figure 19b: The QBO and SAO from the zonal mean zonal wind component from MERRA and ERA-Interim, averaged between 10°S and 10°N.....20

Figure 20a: Global mean precipitation from the most recent set of reanalyses compared against two observational data sets, GPCP and CMAP. The times of introduction of AMSU-A on NOAA-15 and NOAA-16 are shown, along with the timing of the removal of AMSU-A on NOAA-16 because of instrument failure.....21

Figure 20b: Global mean analysis increment of moisture inferred from the imbalance between evaporation and precipitation, from ERA-Interim (red), JRA-25 (orange), MERRA (green), and CFSR (purple).....21

Figure 21: The annual cycle of the global mean precipitation, evaporation, and their difference, from MERRA. The pre-AMSU era is shown in green and the post-AMSU era in cyan.....22

Figure 22a: Temperature anomalies at 2m (K) calculated relative to the 1989-1998 mean. The time series from ERA-40 and ERA-Interim are compared against the CRUTEM3 observations (Brohan et al., 2006). The topmost panels are the time series of 12-month running global average anomalies. The top left-hand panel is the time series from anomalies sampled according to availability of CRUTEM3 data (see lower set of panels); the top right-hand panel is from the raw time series.....22

Figure 22b: The annual global mean 2-m temperature over land in NCEP-NCAR R1 (green), CFSR (red), and GHCN-CAMS (blue) over the period of 1979–2009. Units: K. Least squares linear fits of the three time series against time (thin lines). The linear trends are 0.66, 1.02, and 0.94 K (31 yr)⁻¹ for R1, CFSR, and GHCN-CAMS, respectively. (Note that straight lines may not portray climate change trends accurately).....23

Figure 23: Global mean temperature anomalies (K) in the middle stratosphere from ERA-Interim (blue) and MERRA (red). Data are shown for 5hPa (top) and 10hPa (bottom). The anomalies are computed from the mean annual cycle in 2000-2010 for each individual analysis.....23

Figure 24: Global mean precipitation (mm day⁻¹) for the available reanalyses compared against two observational data sets, GPCP and CMAP.....24

Figure 25: Time series of the 6-hourly first guess (blue curves) root-mean-square (RMS) difference from pressure observations and (red curves) expected RMS difference calculated over separate years from 1870 to 2008 for the (a) northern hemisphere (20°N-90°N) and (b) southern hemisphere (20°S-90°S). The square root is calculated on the annual mean square values. The thin black curve shows the average number of pressure observations for each analysis in the indicated year (note the logarithmic scale).....27

Figure 26: Globally averaged bias estimates (K) for AMSU-A channel 6 radiances from NOAA-15, -16, -17 and Aqua based on ERA-Interim (from Dee and Uppala (2009), top) and MERRA (bottom). The bias estimates based on a 12-hourly assimilation cycle in ERA-Interim and a 6-hourly assimilation cycle in MERRA.....28

Figure 27: Globally analysis departures (K) and observation counts for radiosonde observations at 200 hPa based on MERRA (top) and ERA-Interim (from Dee and Uppala (2009), bottom). Observation counts represent 12-hour totals in ERA-Interim and 6-hour totals in MERRA.....29

1. Introduction

Between early 2009 and early 2010, four new global atmospheric reanalyses became available for scientific research: ECMWF's ERA-Interim reanalysis (Dee et al., 2011a, b), NASA's Modern-Era Retrospective analysis for Research and Applications (MERRA, Rienecker et al., 2011), NCEP's Climate Forecast System Reanalysis (CFSR, Saha et al., 2010) and the NOAA-CIRES Twentieth Century Reanalysis (20CR, Compo et al., 2011). In addition, the JMA began production of a new global reanalysis (JRA-55, Ebita et al., 2011). With so much recent experience being focused on the methodologies and technologies of reanalyses, it seemed an opportune time to gather the primary developers for a meeting to review the system advances and lessons learned from the evaluations of the reanalyses. Thus, in April 2010, developers representing each of the major reanalysis centers met at NASA Goddard Space Flight Center. The meeting included overviews of each center's development efforts, a discussion of the issues in observations, models and data assimilation, and, finally, identification of priorities for future directions and potential areas of collaboration. This report summarizes the deliberations and recommendations from the meeting as well as some advances since the workshop.

2. Major System Advances

The earlier generations of reanalyses from NCEP and ECMWF have proven to be extremely valuable scientific tools, enabling climate and weather research not otherwise possible. They continue to be used, even with their known flaws, because of the information content and form of the products: regular, gridded meteorological fields based on observations. The community of users has a broad array of needs, but those needs seem to be well met by time series of such gridded fields that are of long duration and that are kept current.

Individual centers have their own objectives, depending on their mission (see Appendix A), in preparing these newest reanalyses. However, the primary rationale is the availability of new systems or updates to older systems that make some significant progress in addressing deficiencies in NCEP-NCAR R1 and ERA-40, especially in terms of the hydrological cycle and treatment of biases in satellite observations. Here we briefly summarize advances made in models, analysis/assimilation systems, and the treatment of observations.

2.1 Model

The models used in the latest reanalyses are not very different from those used, for example, for ERA-40 or NCEP-DOE R2. Of course there have been updates in the tuning of parameterizations as new satellite observations, especially from the NASA EOS series, have provided new information and insight on cloud properties and moisture distributions. Perhaps the most significant development has been the implementation of prognostic cloud schemes, which have also facilitated updates to the use of moisture observations during assimilation. The inclusion of prognostic ozone has also allowed the assimilation of ozone retrievals; in MERRA the ozone analysis also has a radiative impact. Additionally, the higher horizontal and vertical resolution and extension of the vertical domain have been important for better representation of transports.

2.2 Analysis and Assimilation

The analysis schemes used in the current generation of reanalyses have been improved in several ways compared with their first-generation predecessors. ERA-Interim (see A.2) and JRA-55 (see A.5) use four-dimensional variational (4D-Var) algorithms, which take the time dimension into account explicitly as observations are used during the assimilation window. This involves not only computing the observation-minus-background state departures at the “correct” time of the observations, but also using the forecast model to propagate the influence of the observations through time in a dynamically consistent manner. This is likely to be of increased importance during the satellite era in which large numbers of observations are available on a near-continuous basis.

MERRA (see A.1) and CFSR (see A.3) use a 3D-Var algorithm based on the Grid-point Statistical Interpolation (GSI) scheme jointly developed by NCEP and GMAO, which also includes a number of advancements over 3D-Var algorithms used previously. In particular, the observation-minus-background departures are computed with increased temporal accuracy, and a dynamic constraint on noise is employed to improve the balance properties of the analysis solution. In MERRA, an incremental analysis update (IAU) procedure is also used in which the analysis correction is applied incrementally to the forecast model through an additional tendency term in the model equations. This has ameliorated the spin-up problem with precipitation during the very early stages of the forecast and greatly improved aspects of the stratospheric circulation.

The 20CR (see A.6) is unique in its use of an ensemble Kalman filter (EnKF) to reanalyze observations of surface pressure from 1871 to the present time. A well-known advantage of the EnKF is that the background error covariances evolve dynamically from one assimilation time to the next. The technique is especially well suited for problems involving a sparse observing network (in which accurate extrapolation of the available observational information to unobserved locations becomes critical), or an observing network that changes substantially during the course of the reanalysis (so that the background errors reflect the associated changes in the accuracy of the background forecast). Both aspects are of primary importance in 20CR.

Except for 20CR, the current reanalyses make extensive use of satellite radiance information, including the hyper-spectral data from AIRS. Successful use of these data requires careful quality control and bias correction procedures that are channel-specific. The bias in a given satellite channel can vary significantly in space and time depending on the atmospheric conditions, systematic errors in the radiative transfer model, and quality and age of the instrument. In most data assimilation schemes, the bias in each satellite radiance measurement is represented by a linear predictor model in which a relatively small number (~10) of parameters is used to describe these and other related dependencies. In the first-generation reanalyses that used satellite radiances, including ERA-40 and JRA-25 (see A.4), these parameters were estimated separately for each channel using an offline procedure based on a reference data set.

In the current reanalyses, bias estimation is performed automatically during the data assimilation procedure using a variational bias correction (VarBC) scheme, which was originally developed for numerical weather prediction at NCEP (Derber and Wu, 1998). The bias parameters are updated each analysis cycle by including them in the control vector used to minimize the analysis cost function. This ensures that the bias estimates are continuously adjusted to maintain consistency between the bias-corrected radiances and all other information used in the analysis,

including conventional observations and the model background state (Dee and Uppala, 2009, henceforth DU09). An important technical advantage of this approach is that it removes the need for manual tuning and other interventions as the satellite observing system changes over time. The bias estimates also adapt in response to natural phenomena that can severely affect the radiance measurements, such as the Mt. Pinatubo eruption in 1991 (e.g., Figure 1, from DU09). The use of variational bias correction thus represents one of the most important advancements in the assimilation methodology of the current generation of reanalyses.

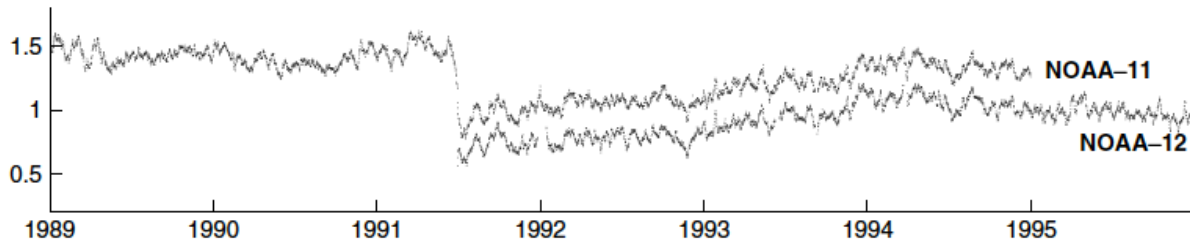


Figure 1: Tropical averages (20°S-20°N) of 12-hourly variational bias estimates (K) for HIRS channel 11 radiance data from NOAA-11 and NOAA-12 in ERA-Interim. [From Dee and Uppala (2009)]

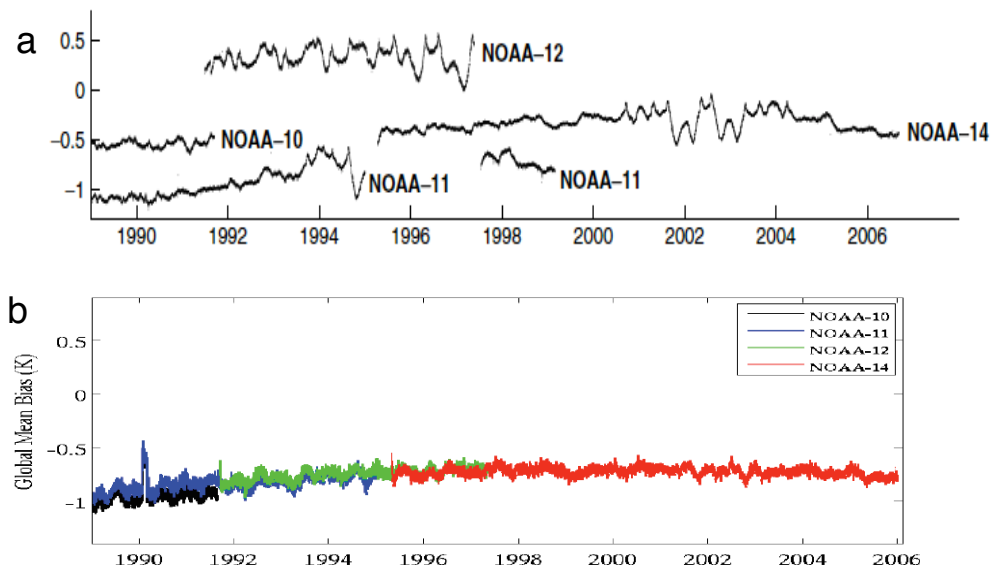


Figure 2: Global mean 12-hourly variational bias estimates (K) for MSU channel 2 radiance data from NOAA-10, NOAA-11, NOAA-12, and NOAA-14. The upper panel is from ERA-Interim (from Dee and Uppala, 2009); the lower panel is from MERRA. The latter uses MSU data from NOAA/NESDIS that has been intercalibrated using the simultaneous nadir overpass (SNO) method (Zou et al. 2006).

2.3 Observations

Just as variational bias correction has provided significant benefit to the assimilation of satellite radiances, so have efforts, by data providers and others, to calibrate or reprocess certain observational data sets improved their usefulness in the current reanalyses. In terms of satellite observations, the Microwave Sounding Unit (MSU) on board NOAA-10, -11, -12 and -14 provides one of the longest records of remotely sensed atmospheric temperature from a single sensor type, extending from 1978 – 2007 with overlapping lifetimes of up to three years between satellites. In the original data sets, the global mean bias estimates for the same MSU channel on different satellites differ by up to a degree or more (Figure 2a), limiting the usefulness of these data for climate-change research and possibly having a negative effect in the variational bias correction scheme. NOAA/NESDIS has begun recalibrating observations from MSU and other instruments using a simultaneous nadir overpass (SNO, e.g., Zou et al., 2006) method. The recalibrated radiances for MSU channels 1 – 3 have been assimilated in MERRA, and exhibit near-uniform biases with a discernible upward trend over the length of the data record (Figure 2b).

Another important observational item worthy of mention is the treatment of radiosonde data since these data continue to have a major impact on global analyses. In addition to the radiation bias correction that all reanalyses apply to radiosonde temperatures to account for changing solar effects on the thermistor, MERRA and ERA-Interim applied some additional pre-processing corrections. Corrections for MERRA include the removal of large time-mean temperature differences in radiosonde observations collected at 00 and 12 UTC with the Vaisala RS-80 instrument. The differences occur as a result of a coding error in the post-processing software at the observing stations, and primarily affect observations in the stratosphere (Redder et al., 2004). The homogenization scheme of Haimberger (2007) was then applied to radiosonde observations (until 2005), with updated values consistent with the Vaisala RS-80 corrections described above. ERA-Interim and JRA-55 also applied Haimberger’s homogenization correction, but using the correction developed without the prior correction of Vaisala RS-80 data. Finally, since those pre-processing corrections were made for MERRA, the radiation bias correction applied to radiosonde temperature observations was modified so that it could still account for seasonal changes in the solar elevation angle that affect the thermistor even in the presence of the other corrections.

3. Quality of the Reanalyses

In this section, we provide an assessment of the extent to which the system advances noted above have led to measurable improvements in the reanalysis products. We briefly look at several, mostly climate-oriented, metrics that can be used to evaluate the quality of the reanalyses. The view includes both improvements over the previous generation of analyses and remaining deficiencies. For the former, we highlight major improvements regardless of whether or not they occur in all the reanalyses; for the latter, we attempt to highlight the problems that are common to these products. In this way we hope to avoid focusing on problems that are specific to any one system, while emphasizing the capabilities and promises that current reanalysis technologies can offer the climate community.

A basic question is how to measure the quality of reanalysis products. The discussion below is organized around four types of metrics: (1) the quality of forecasts made from the analyzed states, which itself requires appropriate metrics; (2) climate-related diagnostics with comparisons against observation-only based products; (3) the magnitude and nature of analysis increments, particularly systematic corrections that are required to keep the assimilation close to the observed trajectory and affect the energy and water budgets of the atmosphere; and (4) the sensitivity of the product to changes in the observing system, which is particularly important if the reanalyses are to be useful in assessing climate change.

3.1 Evaluations through weather forecast skill

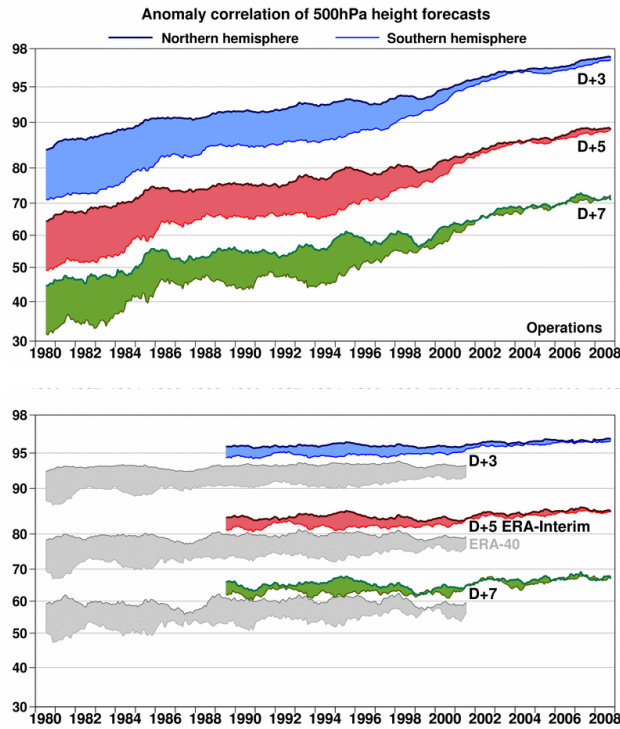


Figure 3a: Extratropical anomaly correlations for 3-, 5-, and 7-day forecasts of 500 hPa height based on the ECMWF operational forecast system (top) and the ERA-Interim and ERA-40 reanalyses (bottom), after Dee and Uppala (2009).

The generation of new retrospective analyses of historical meteorological data has been driven by the steady improvements of the data assimilation systems used for operational weather predictions. Modern systems are capable of extracting much more information from earlier data than the systems that were operational at the time the observations were taken. This effect is dramatically illustrated in Figure 3a (from DU09), which shows how the forecast skill of the operational ECWTF system has improved over time (upper panel), as compared with the forecast skill when more recent ECMWF systems are used to re-analyze the historical observation (lower panel). Since both operational and reanalysis forecasts are based on

practically¹ identical observation streams, the difference between the two can be attributed almost solely to improvements in the data assimilation system – better models and better analysis techniques. Conversely, it is interesting to note (lower panel) the role of the improving observing system in allowing more accurate forecasts, especially during the last decade.

Improving the accuracy of an analysis is a central concern of the numerical weather prediction community as a means of achieving improved forecast skill. In the case of climate reanalyses, it can be debated whether improving accuracy (and therefore forecast skill) should receive priority over other improvements such as temporal consistency (see section 3.3). It is clear, however, that accuracy is nevertheless an important property of reanalyses, impacting the quality of the first guess fields, as well as the physical consistency of the products (in the sense of having smaller analysis increments – discussed further below). Figure 3a shows how the ERA-Interim product has benefitted from the recent improvements to the operational model and analysis system, showing essentially modern-day skill levels extending back to the late 1980s where they are substantially above the operational skill levels of that time. Figure 3b shows the same for NCEP reanalyses versus operations. Such improvements highlight the benefits of reanalyzing earlier periods with a fixed modern-day data assimilation system (including improved observations) to address, at least in part, consistency of the products in time in the face of a changing observing system.

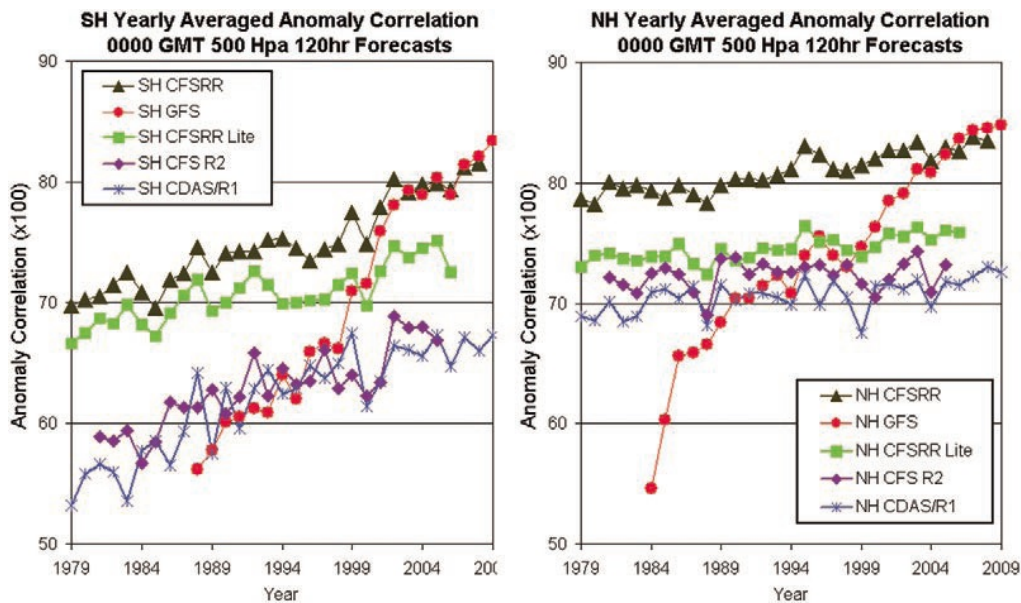


Figure 3b: Yearly averaged (left) Southern Hemisphere and (right) Northern Hemisphere 00 UTC 120-h forecast anomaly correlations for CFSR (black triangles), operational GFS (red circles), CFSR-Lite (green squares), CFS R2 (purple diamonds), and CDAS R1 (blue stars).

¹ Two caveats are that (1) the observations used for reanalysis are often “cleaned-up” versions of the real-time streams and may include some additional data, and (2) as time progresses, an aging reanalysis system may be technically unprepared to assimilate new observing systems.

3.2 Climate-related Diagnostics

3.2.1 Water and Energy Cycles

Current models have improved considerably in the representation of the hydrological cycle, and reanalyses have benefited from this. There are still outstanding issues, especially in the representation of precipitation and clouds; however, the quality, measured in terms of bias and spatial structure, of the precipitation has improved substantially in the more recent reanalyses. In fact, the time series of the spatial correlations in Figure 4 show improvements in the earlier years (compare MERRA and CFSR with ERA-40) that further illustrate the benefits of reanalyzing historical observations with an improved data assimilation system. The spatial maps of the bias in the January mean precipitation from the various reanalyses, as estimated with the observation-only Global Precipitation Climatology Project (GPCP, Figure 5a), and the summary Taylor plots (Figure 5b) show that much of the improvement has occurred over the tropical oceans.

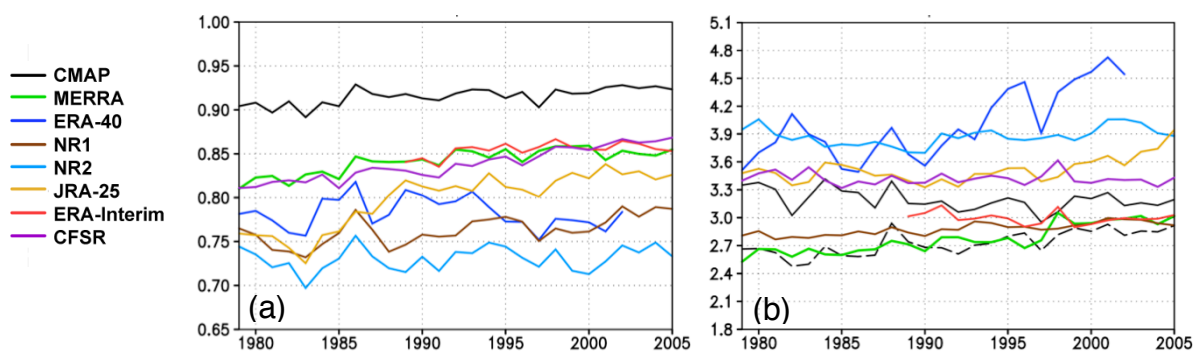


Figure 4: (a) The time series of the spatial correlation of annual mean precipitation averaged over the tropics (15°S-15°N) from several reanalyses and CMAP (black curve) with that from GPCP. (b) The annual mean spatial standard deviation of precipitation (mm day⁻¹) over the tropics. The black dashed line denotes GPCP.

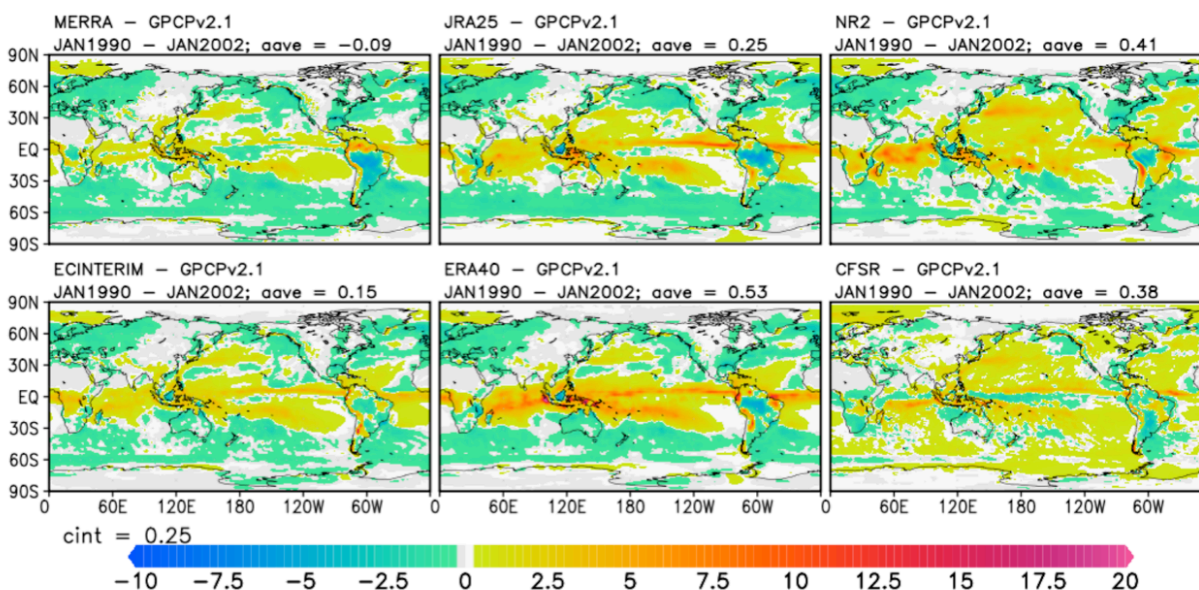


Figure 5a: The precipitation bias (mm day⁻¹) in several reanalyses relative to GPCP, January 1990-2002.

CMAP
 ERA40
 NR1
 NR2
 JRA25
 INTERIM
 CFSR
 MERRA

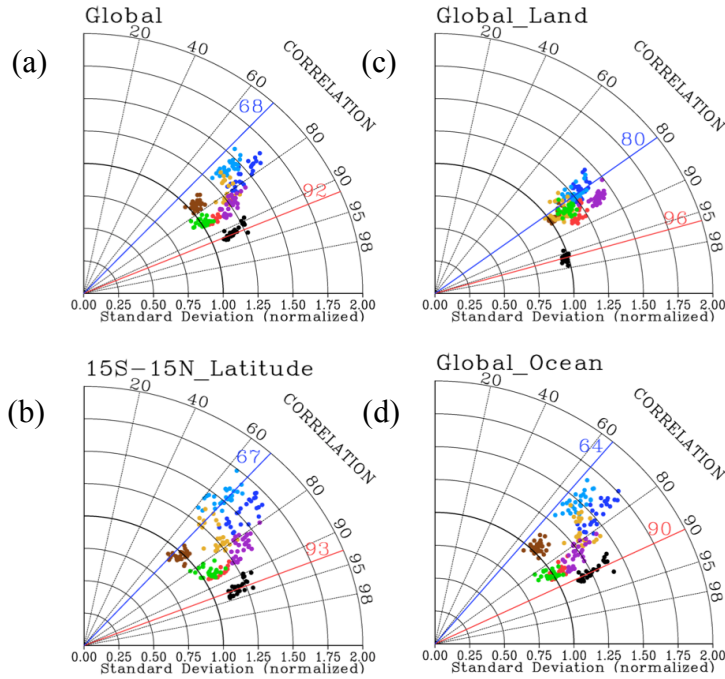


Figure 5b: Taylor diagrams of annual mean precipitation from reanalyses using GPCP as a reference and CMAP as an additional observational reference. Each panel shows the statistics for different regions: (a) globe, (b) tropics, (c) global land, and (d) global oceans. The red and blue lines show limits of expected high and low correlation as determined by comparing GPCP and CMAP observations. See Bosilovich et al. (2008) for details.

Earlier reanalyses were limited in their ability to support water and energy budget analyses, having large biases in the various physical forcing terms (e.g., precipitation, heating rates). “Forcing” fields could only be estimated as a residual of the terms that involved quantities that were strongly constrained by the analysis (e.g., rotational wind) and were less dependent on the model physical parameterizations. In conducting MERRA, emphasis was placed on providing a complete and internally consistent budget including any unphysical terms associated with the analysis increments and other non-physical adjustments (e.g., filtering). For example, Figure 6 shows the various terms in the vertically integrated moisture budget from MERRA, indicating that while the bias (e.g., in precipitation) has been reduced compared to previous reanalyses, the analysis increments nevertheless still contribute substantially to the budget.

Improvements in the representation of clouds remain a challenge that affects the quality of both the water and energy cycles. For example, cloud-related deficiencies are apparent in the joint frequency distribution of long-wave and short-wave fluxes at the top of the atmosphere shown in Figure 7. The joint frequency distribution of these fluxes may be viewed as a two-dimensional histogram that provides an evaluation of the processes that relate temperature, humidity and cloud fields. The latest reanalyses (MERRA and ERA-Interim) appear to have patterns closer to observed (CERES) than the earlier reanalyses (NCEP-DOE R2 and JRA-25), demonstrating the advances made in a general sense regarding the representation of the water and energy cycles.

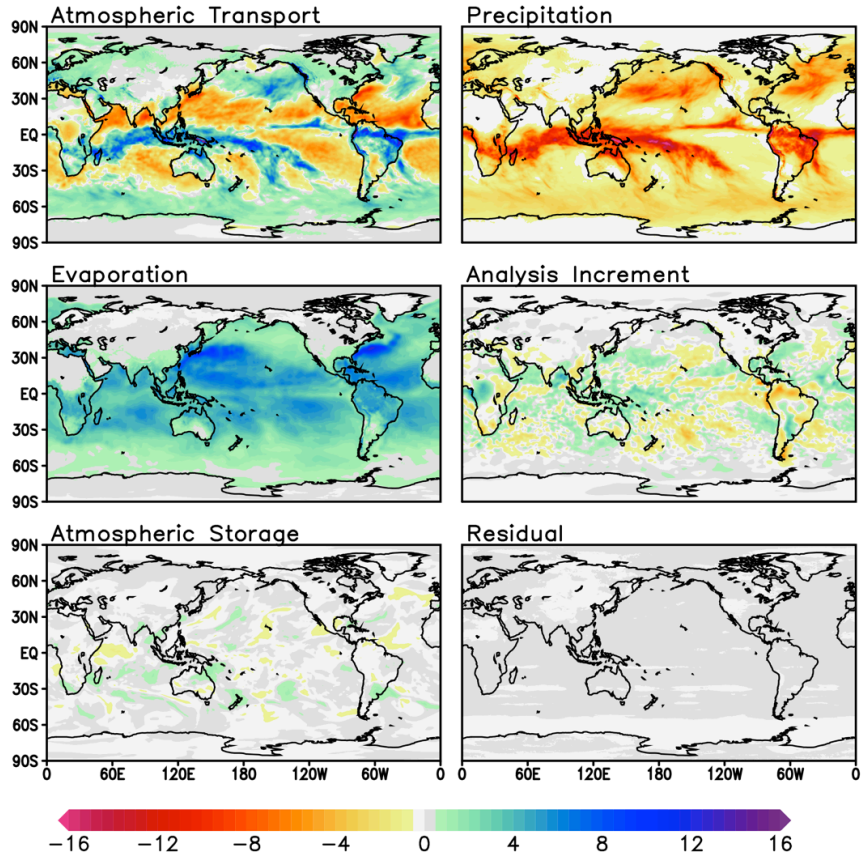


Figure 6: MERRA's estimate of the vertically integrated water vapor budget for January 2004, in $\text{kg m}^{-2} \text{day}^{-1}$.

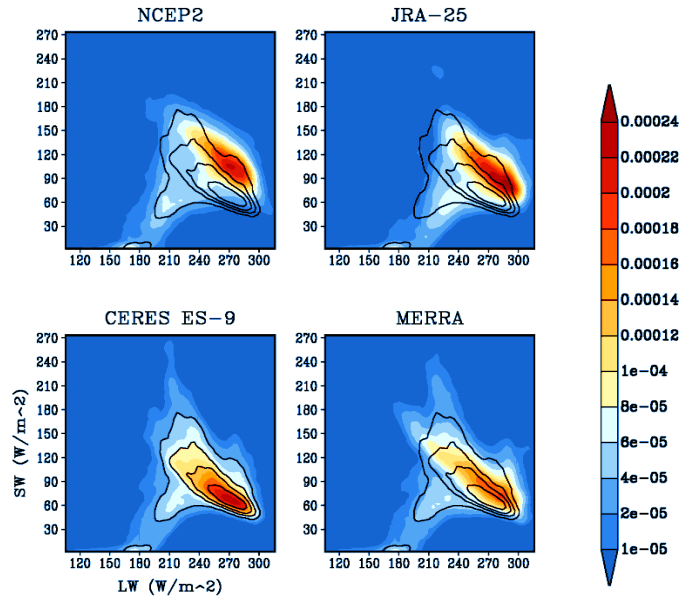


Figure 7: The joint frequency distribution of the top-of-atmosphere long-wave (abscissa) and short-wave (ordinate) fluxes for 2004 from MERRA, NCEP-DOE R2, and JRA-25. For comparison, the results are shown from CERES. The solid line contours from CERES overlay the shaded contours in all panels. [Figure courtesy of Junye Chen]

A summary of the annual and global mean energy flow and balances, estimated from recent reanalyses and compared with an observationally based estimate from Trenberth et al. (2011), is shown in Figure 8. Here, consistency and improvements appear to be greatest at the top of the atmosphere where the net fluxes from the recent reanalyses are all small, while substantial imbalances occur at the surface. The lack of balance at the surface is one of the outstanding problems that continue to limit the use of reanalyses for driving ocean and land models. The primary causes of imbalances are related to the representation of clouds and surface boundary layer processes. Such deficiencies hinder efforts to develop coupled data assimilation systems.

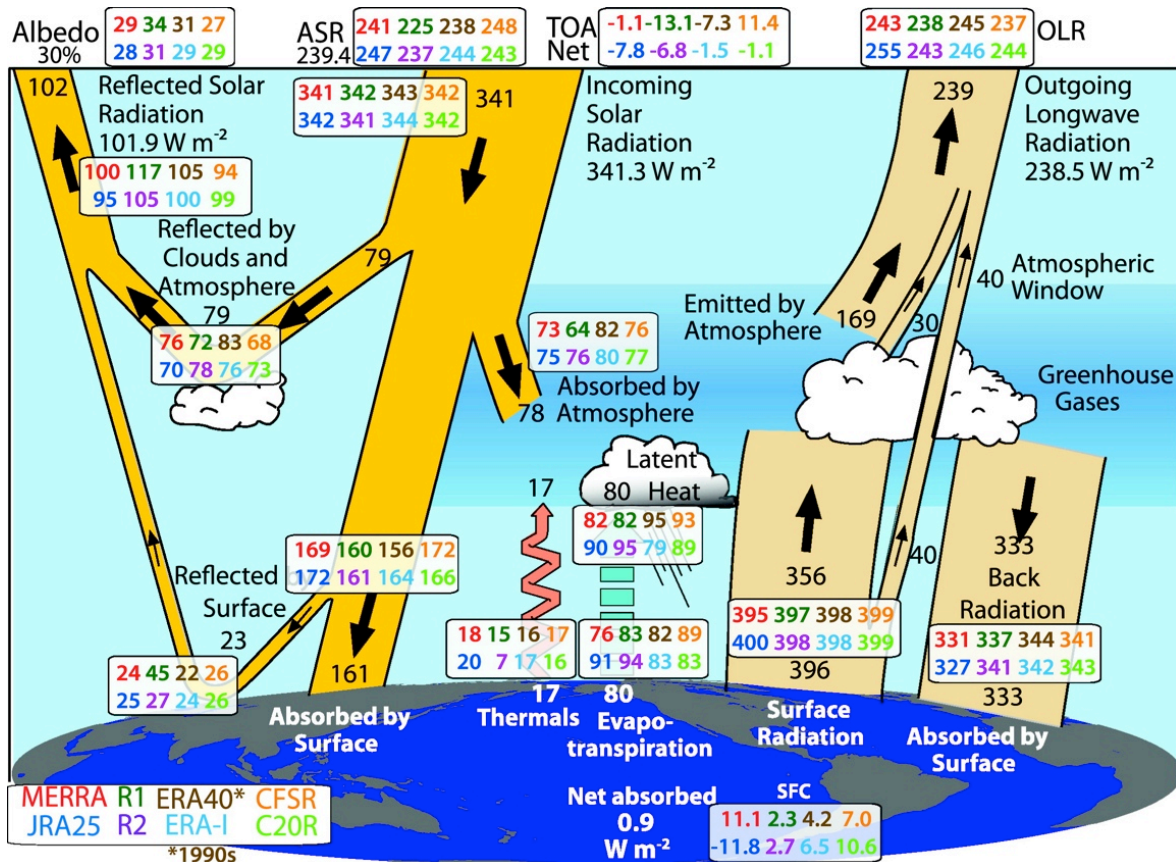


Figure 8: The global energy budget ($W m^{-2}$). The numbers in black and white are those from satellite data climatologies and other observations for the period 2000-2005 from Trenberth et al. (2009). The colored values are from reanalyses for the 2002-2008 period (except ERA40): MERRA (red), NCEP-NCAR R1 (green), ERA40 (brown), CFSR (orange), JRA-25 (blue), NCEP-DOE R2 (purple), ERA-Interim (cyan), and 20CR (green). [From Trenberth et al. (2011)]

Ultimately, studies of water and energy cycle budgets and variability require consistent state estimates of the ocean and land surface. The use of specified SSTs impacts surface flux estimates and limits the consistency of the reanalyses in the surface boundary layer with state estimates elsewhere. Only CFSR, by producing the analysis first guess with their coupled model, allows some degree of interaction between the atmosphere and ocean. One benefit of that is greater consistency between the SST and precipitation fields (e.g., Figure 9).

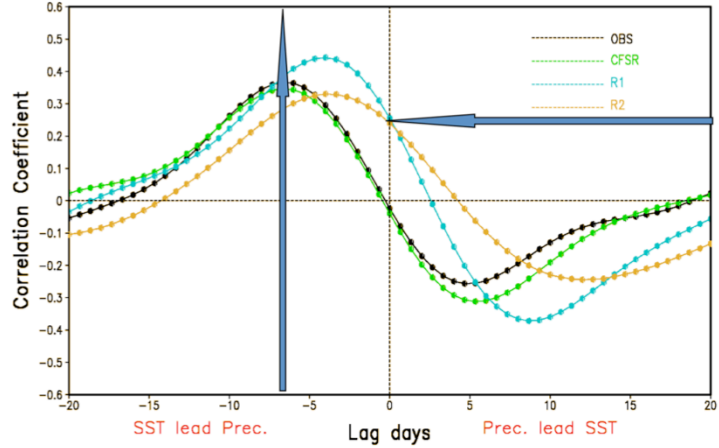


Figure 9: The lag correlation of precipitation and SST for winter over the Western Pacific. The correlation for CFSR is compared with that from observations, NCEP-NCAR R1, and NCEP-DOE R2. Positive lags denote precipitation is leading SST. [From Saha et al. (2010)]

3.2.2 Interannual Variability

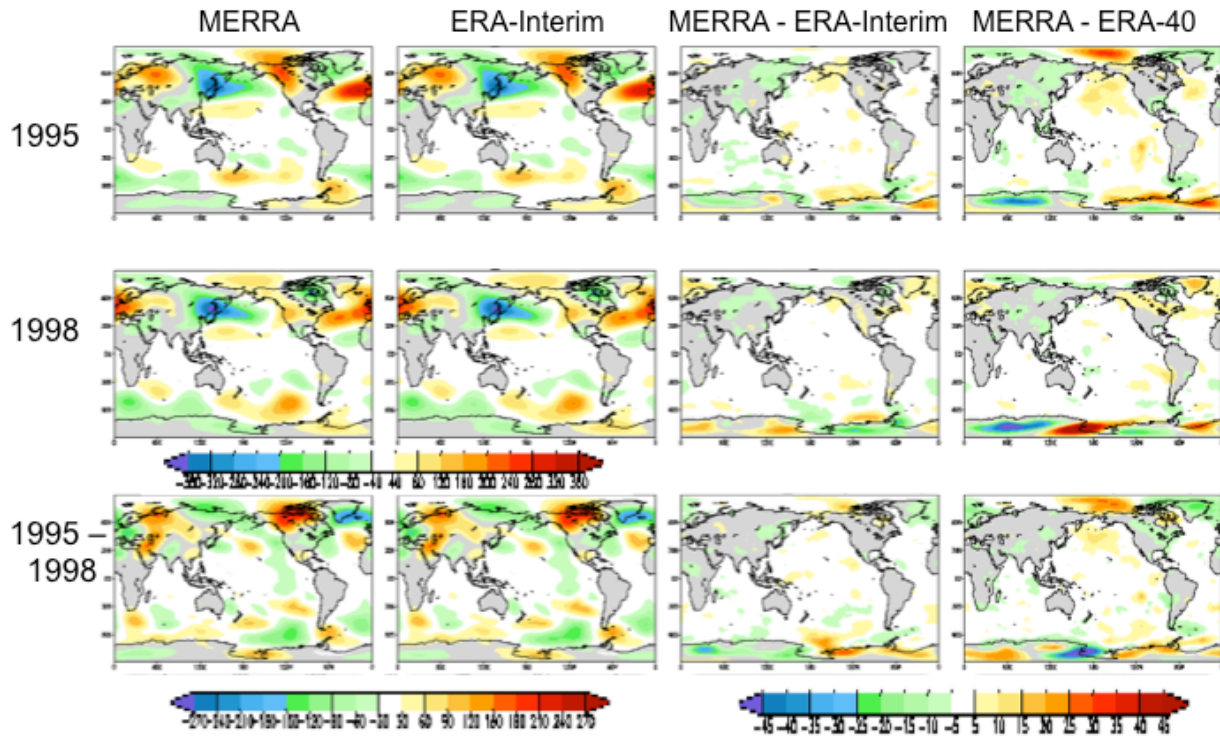


Figure 10: The eddy height field at 300 hPa for January 1995 (upper row) and January 1998 (middle row) from MERRA (first column) and ERA-Interim (second column). The differences between MERRA and ERA-Interim are shown in the third column while the fourth column compares MERRA with ERA-40. The bottom panels show the differences between the two years.

One of the strengths of the most recent reanalyses is the representation of interannual variability; however, the quality is not uniform but depends on both the variable of interest and the location (with primarily vertical and latitudinal dependence). Figure 10 shows, for example, a very high

degree of agreement between the MERRA and ERA-Interim climate anomalies for January eddy height field at 300 hPa as indicated by the difference between monthly-mean analyses for two different years (one a neutral year in terms of the El Niño-Southern Oscillation (ENSO) and one an El Niño year). The differences are much smaller than the amplitude of the El Niño climate signal itself. This agreement is an improvement upon what was already a high level of agreement between MERRA and the ERA-40. Perhaps more surprising is the agreement in higher order moments, such as large-scale atmospheric transports, or in some of the derived fields, such as vertical velocity (Rienecker et al., 2011).

Figure 11 summarizes the correlations of MERRA with observational estimates or, if the latter are unavailable, with ERA-Interim for selected monthly-mean quantities for January. For the eddy height field at 300 hPa, the agreement between MERRA and ERA-Interim is quite high everywhere except for some tropical regions, consistent with the results shown in Figure 10. The global mean of the local correlations is 0.98. While there is also generally close agreement between the two reanalyses of u-wind at 850 hPa, the agreement is lower than that for the eddy field. Some of the lowest correlations occur over tropical land and surrounding regions, including much of the tropical Atlantic. The high correlations of total precipitable water (TPW) in MERRA with the SSM/I estimates over the ocean are not surprising since MERRA assimilated SSM/I radiances. On the other hand, the lower agreement with the specific humidity at 850 hPa from ERA-Interim reflects the large uncertainties in the vertical structure of the moisture field in reanalyses. This, in turn, reflects a lack of strong observational constraints combined with a general sensitivity of the vertical structure of the moisture to the model's convection scheme.

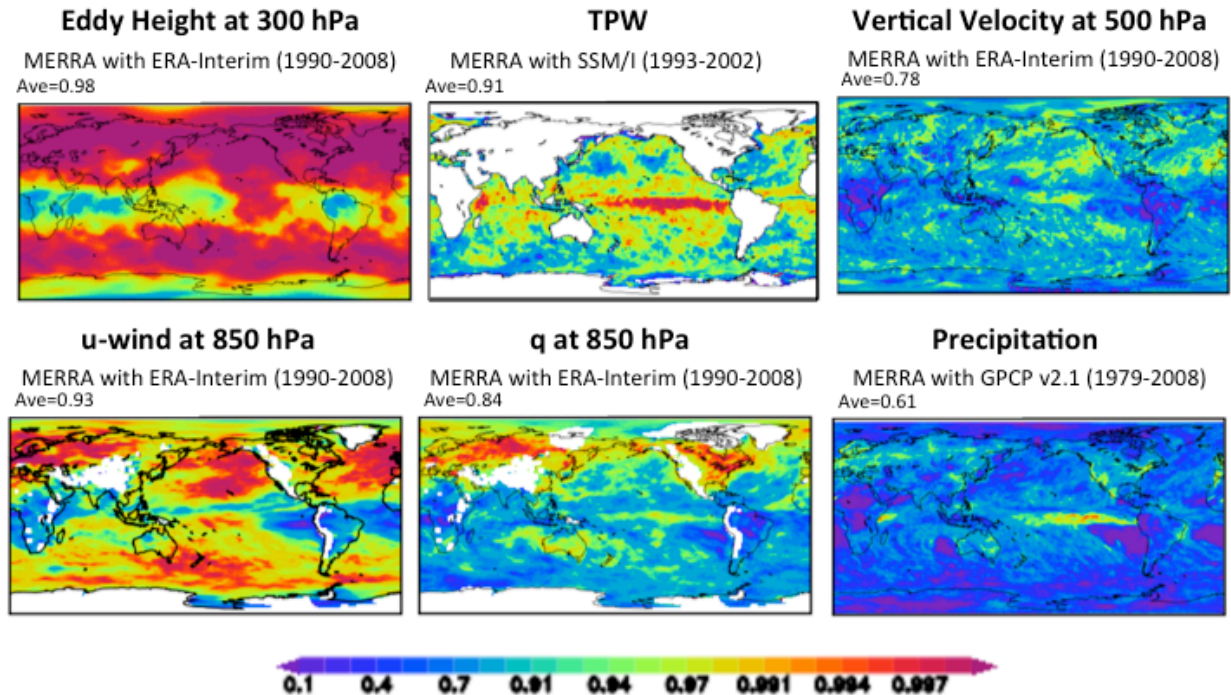


Figure 11: Correlations of MERRA with other estimates of selected monthly-mean quantities in January. The comparisons with ERA-Interim (300 hPa eddy height, vertical velocity at 500 hPa, u-wind at 850 hPa and specific humidity (q) at 850 hPa) are for 1990-2008. The comparison with SSM/I (TPW) is for 1993-2002, and the comparison with GPCP v2.1 (precipitation) is for 1979-2008.

The correlations drop further for quantities related to the divergent wind field (e.g., vertical velocity at 500 hPa) and the hydrological cycle (e.g., precipitation), although though one can find regions where the correlations are quite high, for example, over the tropical Pacific. It should be emphasized, however, that this overall level of agreement is a substantial improvement compared with previous reanalyses (see for example the Taylor plots in Figure 5b).

Figure 12 summarizes results in terms of the zonal mean values of the correlation (R^2) between MERRA and ERA-Interim, and between MERRA and selected observational data sets, for various quantities during January and July. The higher correlations between MERRA and ERA-Interim for precipitation (and OLR), compared with the correlations between MERRA and GPCP, demonstrate the fact that the reanalyses are still more like each other than they are like the observational estimates.

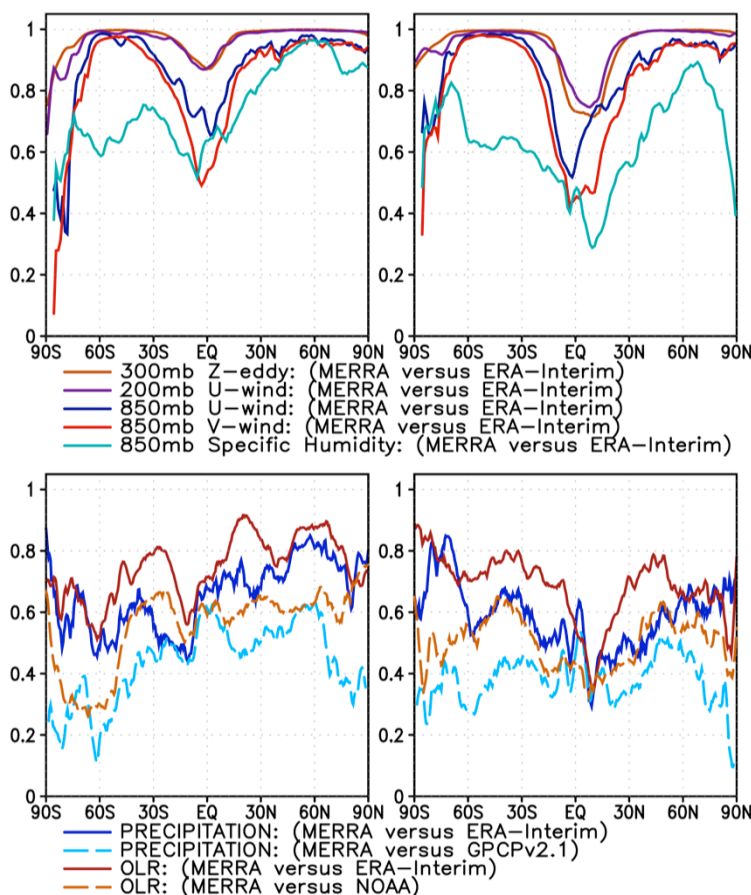


Figure 12: Zonal mean values of the correlation between MERRA and ERA-Interim, and between MERRA and selected observational data sets, for various monthly-mean quantities during January (left-hand panels) and July (right-hand panels) for the period 1990 to 2008. Comparisons with GPCP precipitation and from NOAA’s OLR product are also included. [From Rienecker et al. (2011)]

Compo et al. (2011) provide an assessment of the overall quality of the weather and climate aspects of 20CR. One might suspect that while synoptic and submonthly variability throughout the troposphere could be captured well using only surface observations, lower frequency variability might be more poorly represented (Kanamitsu and Hwang, 2006). However, Figure 13 shows that the patterns of northern hemisphere monthly anomalies of 300 hPa geopotential

height for 20CR correspond well with the ERA-40 and NCEP-NCAR reanalyses. Shown are time series of the pattern correlation between monthly anomalies from 20CR and NCEP-NCAR R1 for the month of December (cyan curve) and June (orange curve). All other months fall between these two extremes. ERA-40 results for December (dark blue curve) and June (red curve) are similar and almost obscure the other curves. The increase of June correlations from an average of 0.84 for the period 1958 – 1978 to an average of 0.89 for 1979 to 2001 most likely reflects the increasing use of satellite observations that reduces the random error in both reanalyses used for comparison. The pattern correlations between 20CR and the upper-air based reanalyses are considerably higher than expected from SST-forcing alone (black curves), suggesting that the surface observation-based reanalysis fields provide useful estimates even of the monthly mean upper-tropospheric fluctuations.

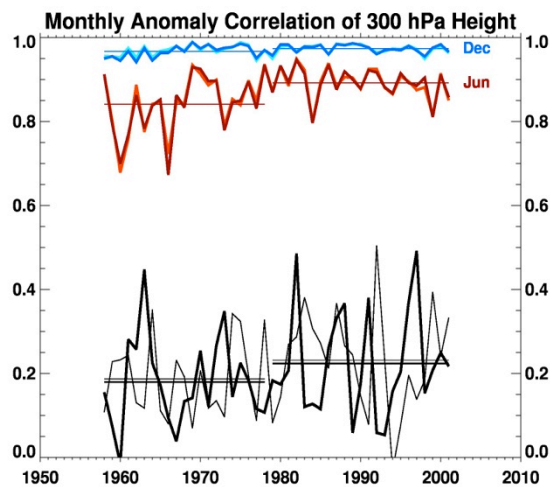


Figure 13: Time series of anomaly pattern correlations between monthly mean anomaly fields of northern hemisphere extratropical 300 hPa geopotential height from two upper-air based reanalyses and 20CR for the months of December (cool colors) and June (warm colors). Correlations with ERA-40 are shown by the blue and red curves. The black curves show the expected anomaly pattern correlations when only the observed SST fields are available for the months of (thick) December and (thin) June using the ECHAM4.5 atmospheric model forced with observed SSTs (courtesy of the International Research Institute). The thin black lines show the mean value of these expected correlations, with the thicker line corresponding to December and the thinner corresponding to June. [From Compo et al. (2011)]

3.2.3 Sub-seasonal and Higher Frequency Variability

There have been significant improvements in the representation of intra-seasonal tropical variability, particularly in the representation of the Madden-Julian Oscillation (MJO) and other convectively coupled equatorial waves. For example, Figure 14 shows wavenumber-frequency diagrams (Wheeler and Kiladis, 1999) for precipitation based on GPCP observations and several reanalyses. When compared against GPCP, the most recent reanalyses (MERRA, ERA-Interim, and CSFR) show clear improvements over the earlier NCEP-NCAR reanalysis in terms of the power associated with the MJO and the lower frequency Kelvin waves.

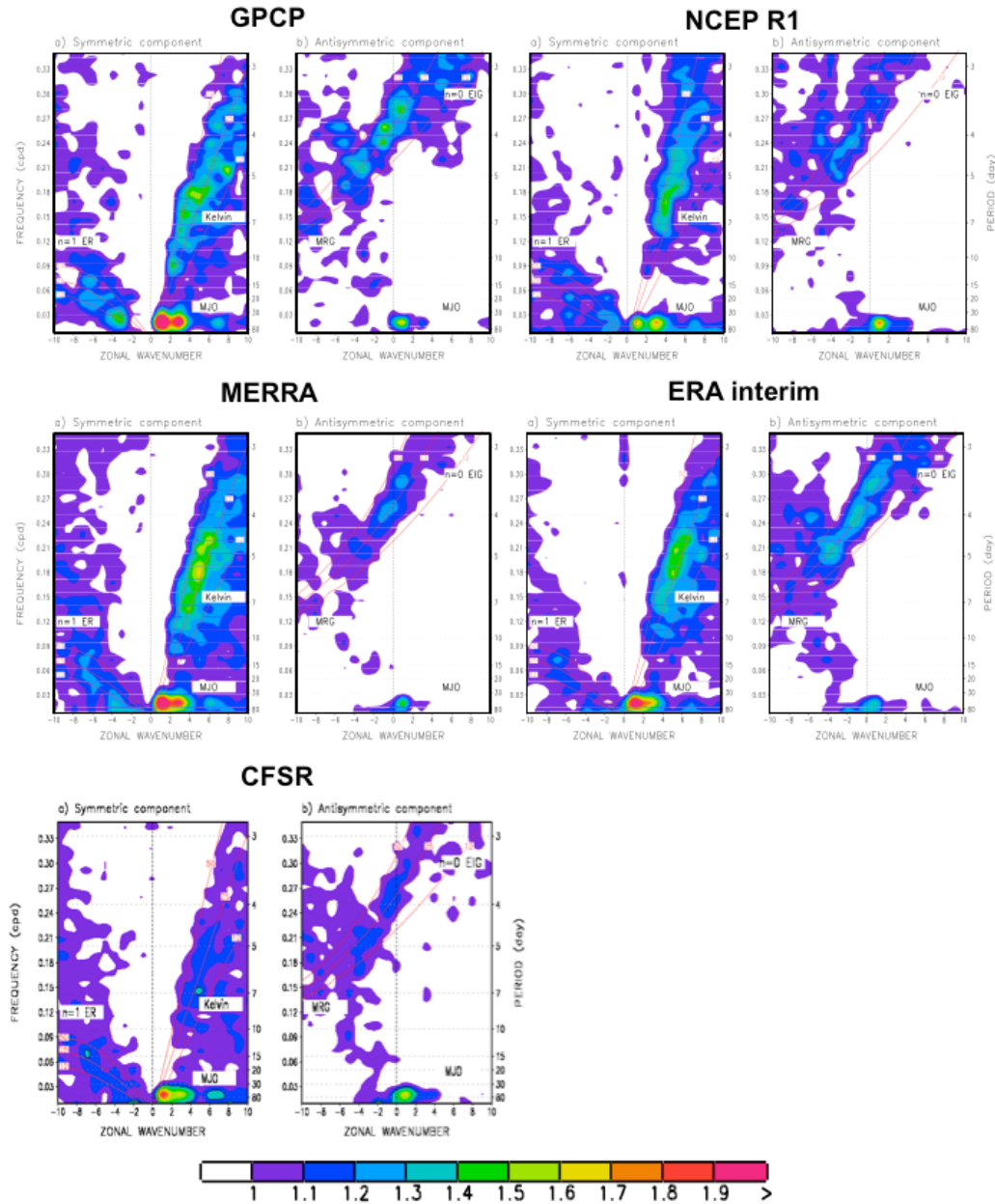


Figure 14: Wavenumber-frequency diagram for precipitation, following Wheeler and Kiladis (1999). ER is equatorial Rossby wave; EIG is eastward inertio-gravity wave, MRG is mixed Rossby-gravity wave. The calculations are based on daily precipitation for 1989-2008 averaged between 15°S and 15°N. For each product, the left-hand panel is the symmetric component and the right-hand panel is the anti-symmetric component.

Reanalyses have traditionally provided good representations of synoptic-scale mid-latitude weather systems (e.g., CCSP, 2008). The recent reanalyses have considerably higher resolution than previous reanalyses and are beginning to provide useful information about the occurrence of tropical storms. For example, Figure 15 shows that tropical storm detection rates in CFSR are quite high for all but the eastern Pacific. In addition to enhanced resolution, this result also likely reflects the application of a tropical storm relocation procedure prior to performing the analysis.

On the other hand, the most intense storms (for example, category 4 and 5 hurricanes) are still not well represented (see, e.g., Figure 16).

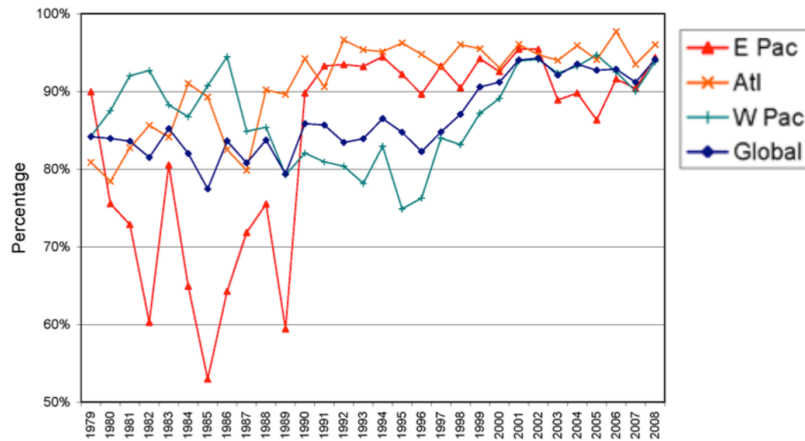


Figure 15: Tropical cyclone detection rate from CFSR. [From Saha et al. (2010)]

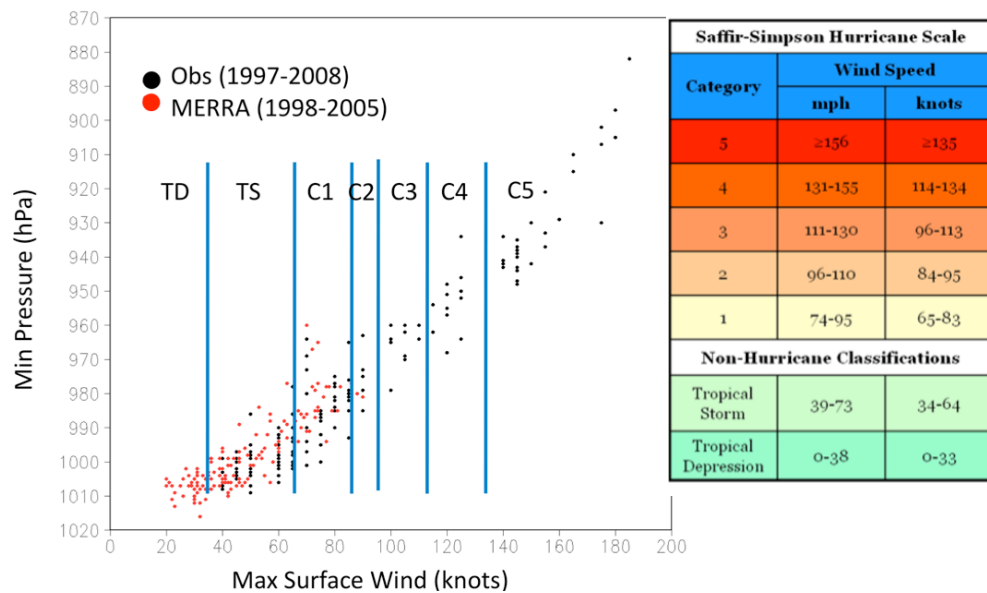


Figure 16: Maximum intensity of tropical storms in the Atlantic detected in MERRA over the period 1998-2005, compared with observations from 1997 to 2008.

While there has been significant improvement in the representation of variability on time scales shorter than one season, there has been little or no improvement in the representation of the diurnal cycle. For example, while the global distribution of the amplitude of the diurnal cycle in precipitation is generally reasonable, all reanalyses suffer from incorrect phasing, especially during the warm season over land areas where local phenomena such as low level jets and mesoscale convective systems, together with complicated/high terrain, can play an important role in determining the timing of rainfall (Figure 17). Deficiencies in the diurnal cycle (e.g., the timing of precipitation and clouds) have important impacts on the quality of land hydrology, contributing to unrealistic soil moisture and evaporative fluxes.

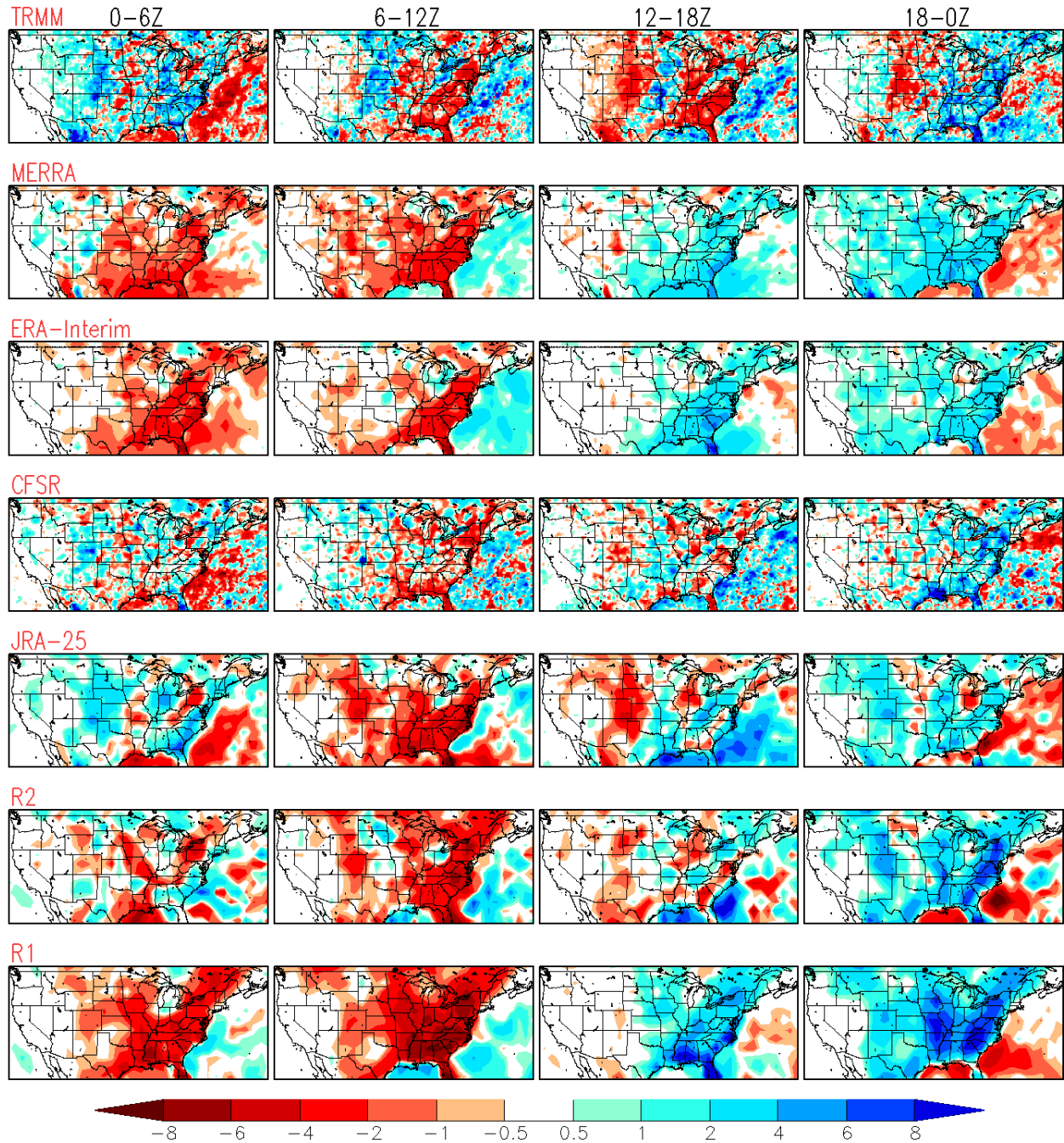


Figure 17: Diurnal variation in precipitation (mm day^{-1}) over the United States for July 2004. The July mean has been removed. Results are shown as 6-hour averages for TRMM observations, and for the reanalyses: MERRA, ERA-Interim, CFSR, JRA-25, NCEP-DOE R2, and NCEP-NCAR R1.

A global examination of the synoptic quality of the 20CR fields is made by comparing the geopotential height fields with available reanalyses that included upper-air and satellite observations, such as ERA-40 (Uppala et al., 2005). Even in the upper-troposphere, the quality

of the surface-pressure based 20CR is high, as shown by the correlation of 300 hPa geopotential height anomalies from 20CR with the ERA-40 (Figure 18).

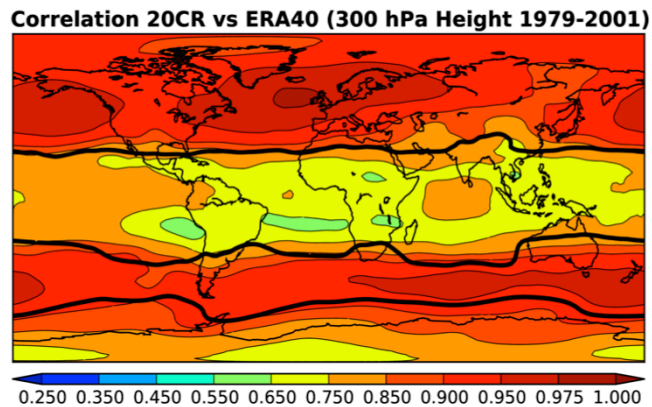


Figure 18: Map of the local anomaly correlation between four-times daily anomalies of 300hPa geopotential from ERA-40 and 20CR for the period 1979 – 2001. The thick black line contour indicates the region where ERA-40 and NCEP-NCAR R1 correlate highly (0.975) in this quantity during this period. [From Compo et al. (2011)]

3.2.4 The Stratosphere

The dominant components of the climate and variability in the lower stratosphere over the Arctic were represented quite well in early analyses produced with low model tops (e.g., Pawson and Fiorino, 1998a) since the large-scale structure in this region is sampled by radiosondes. Even in the Antarctic, temperature retrievals from space-based data were adequate to constrain the polar vortex structure, but early analyses do not capture low temperatures characteristic of the polar regions. Increasing the height of the upper boundary led to substantial improvements in the analyzed structure of the middle stratosphere in ERA-40, ERA-Interim and GEOS-5 compared to the earlier products. These model improvements coupled with improved use of space-based radiance observations have led to consistent and accurate analyses of the middle and polar latitudes in both hemispheres, up to altitudes of 30-40 km.

At higher levels, even the most recent analyses are less successful. Manney et al. (2008) demonstrated that structures in the upper stratosphere and mesosphere are not well captured in analyses performed using systems that assimilate only nadir-sounding radiance observations. It has also been shown that the application of variational bias correction does not work well in the upper stratosphere, where the only data sources are deep-layer radiances from AMSU-A Channel 14 or SSU, and the underlying models typically have large and fast-growing biases (e.g., Rienecker et al., 2011). Successful application of variational bias correction relies on the availability of a range of near-independent measurements with different (random) biases and also factors in the model state: this fails in the stratopause region because of persistent systematic model errors and the absence of a range of observations.

In the tropics, the quasi-biennial oscillation (QBO) was captured by earlier reanalyses, as in Figure 19a, but with important departures from observations. The differences largely concern the strength of the winds at the various levels and the timing of the transitions between regimes

(Pawson and Fiorino, 1998b). Reasons for this are not entirely clear, although Gaspari et al. (2006) showed that adequately long length scales are needed to spread wind information from sparse radiosondes around the globe, and that inadequate data selection can readily lead to good observations being rejected in favor of poor analyses in the tropical stratosphere. ERA-40 analyses of the QBO are in excellent agreement with observations, to the extent that these are used as pseudo-observations in CFSR. ERA-Interim and MERRA show very realistic zonal wind variability associated with the QBO (Figure 19b). There is less agreement about tropical winds in the upper stratosphere, dominated by half-yearly wind oscillations, where no direct constraints are available and the issues associated with model bias and the availability of deep-layer radiance observations are major factors.

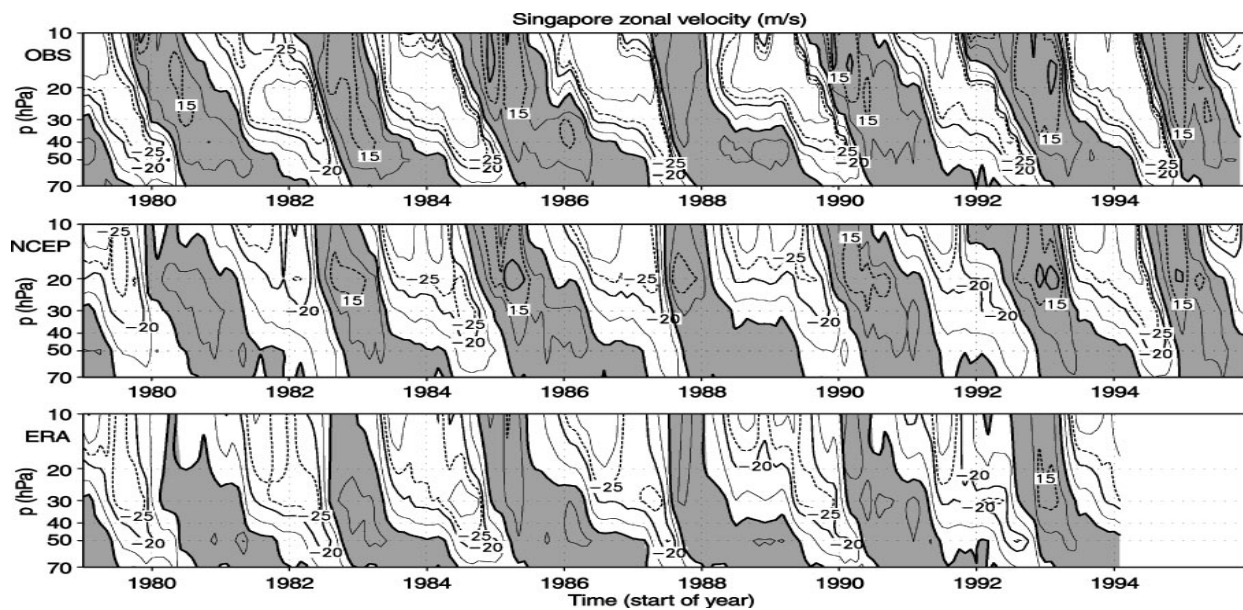


Figure 19a: Time series of the monthly mean zonal velocity at Singapore from (*top*) rawinsonde observations, (*center*) NCEP-NCAR R1, and (*bottom*) ERA-15. The contour interval is 10 m s^{-1} , the 15 m s^{-1} and 25 m s^{-1} are also included (*dashed*) and positive values (i.e. westerlies) are *shaded*.

Stratospheric applications of reanalyses include computations of trace gas transport, which are strongly sensitive to the strength and structure of the Brewer-Dobson circulation. Meteorological analyses performed in the 1990s typically showed an over-strong Brewer-Dobson circulation, with excessive tropical ascent and high-latitude descent (e.g., Douglass et al., 1996), leading to unrealistically low (high) values of tropical (polar) ozone columns. In the early 2000s, analyses tended to transport trace gases in an over-dispersive manner (e.g., Schoeberl et al., 2003 or Tan et al., 2004), leading to excessively young mean age of air and unrealistic age spectra. In the middle 2000s, the introduction of time smoothing techniques led to more realistic ozone transport computations and mean age of air distributions (e.g., Pawson et al., 2007). Monge-Sanz et al. (2007) showed successive improvements in stratospheric transport computed from ECMWF analyses that arose from increasing vertical resolution in the stratosphere of the analysis system and ultimately the introduction of 4D-Var.

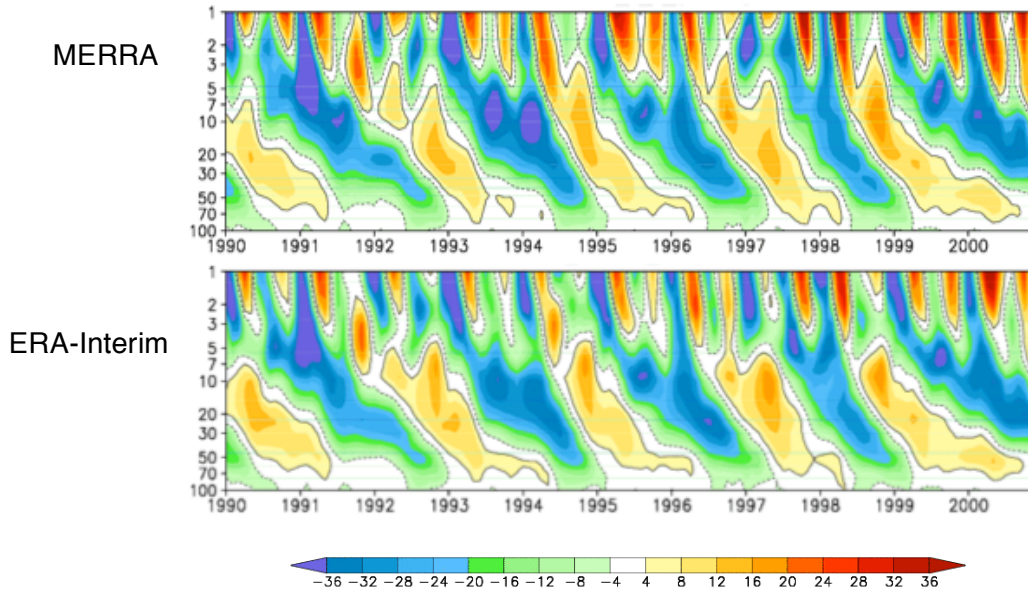


Figure 19b: The QBO and SAO from the zonal mean zonal wind component from MERRA and ERA-Interim, averaged between 10°S and 10°N.

Regardless of these improvements in the Brewer-Dobson circulation, the fact remains that stratospheric transport depends crucially on our ability to represent the slow divergent motion in a system where assimilation constraints are imposed at a frequency consistent with synoptic variations and which is optimized to constrain the rotational component of the flow.

3.3 Trends and Long-term Variability

All reanalyses are affected by changes in the observing system, especially quantities involving the hydrological cycle (e.g., precipitation and clouds). Such quantities are especially sensitive to changes in moisture data through their impacts on the model convection schemes. Major changes to the observing system – such as the introduction of SSM/I in 1987, AMSU in 1998 and AIRS in 2002 – can produce spurious trends and distort long-term variability. As an example, the time series of global mean precipitation, which is a particularly sensitive measure of changes in the hydrological cycle, shows a number of abrupt changes as well as trends that appear to be linked to changes in the satellite observing system (Figure 20a). The more recent reanalyses, while showing more realistic magnitudes, still suffer from this problem. Interestingly, the “responses” to the observing system changes are very different among the different reanalyses. After the introduction of AMSU-A on NOAA-16, ERA-Interim and MERRA have virtually the same global mean precipitation rate and similar annual cycles. However the time series do not stay synchronized, and, particularly after the demise of AMSU-A on NOAA-16, the two time series depart toward their different pre-NOAA-16 levels. The time series of the inferred analysis increment of moisture (Figure 20b) clearly shows the impact of the changing observing system. The increments in MERRA and CFSR are very highly correlated although their mean values differ.

Spurious shifts in global mean precipitation in ERA-Interim coincide with changes in the number of assimilated rain-affected radiances from SSM/I (Dee et al., 2011, Section 5.2.1). These data were assimilated using an early version of the 1D+4D-Var retrieval scheme, which introduced a

net drying effect into the reanalysis (Geer et al., 2008). On the other hand, there are no discernible changes in mean precipitation in ERA-Interim that can be related to the use of AMSU or SSM/I clear-sky radiance data.

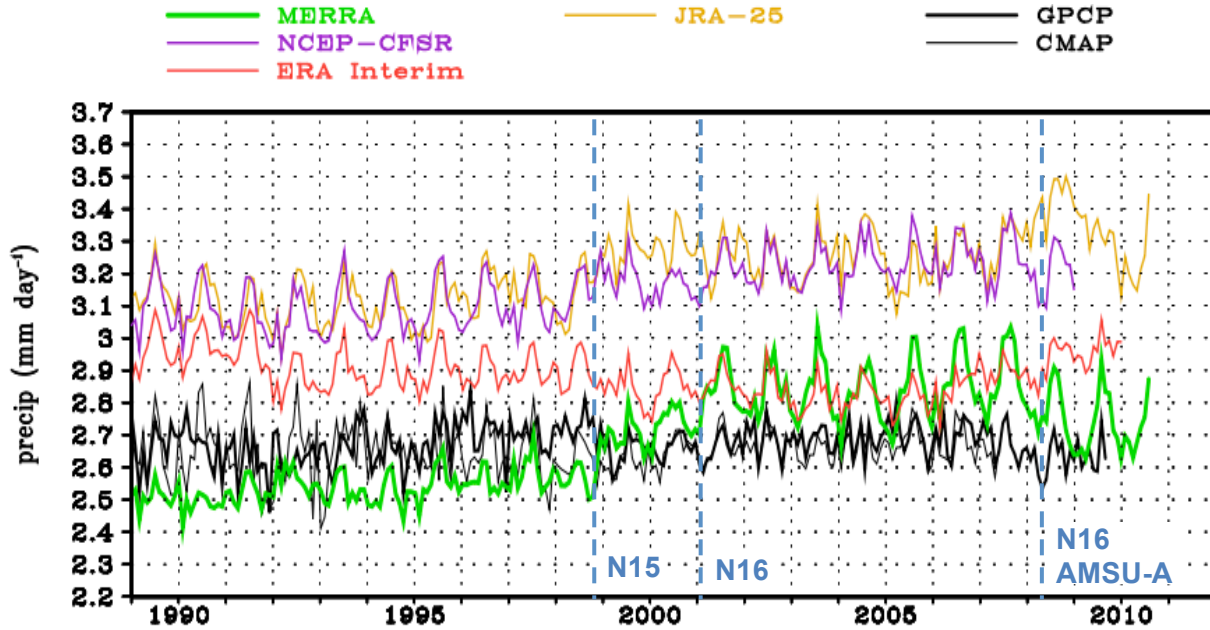


Figure 20a: Global mean precipitation from the most recent set of reanalyses compared against two observational data sets, GPCP and CMAP. The times of introduction of AMSU-A on NOAA-15 and NOAA-16 are shown, along with the timing of the removal of AMSU-A on NOAA-16 because of instrument failure.

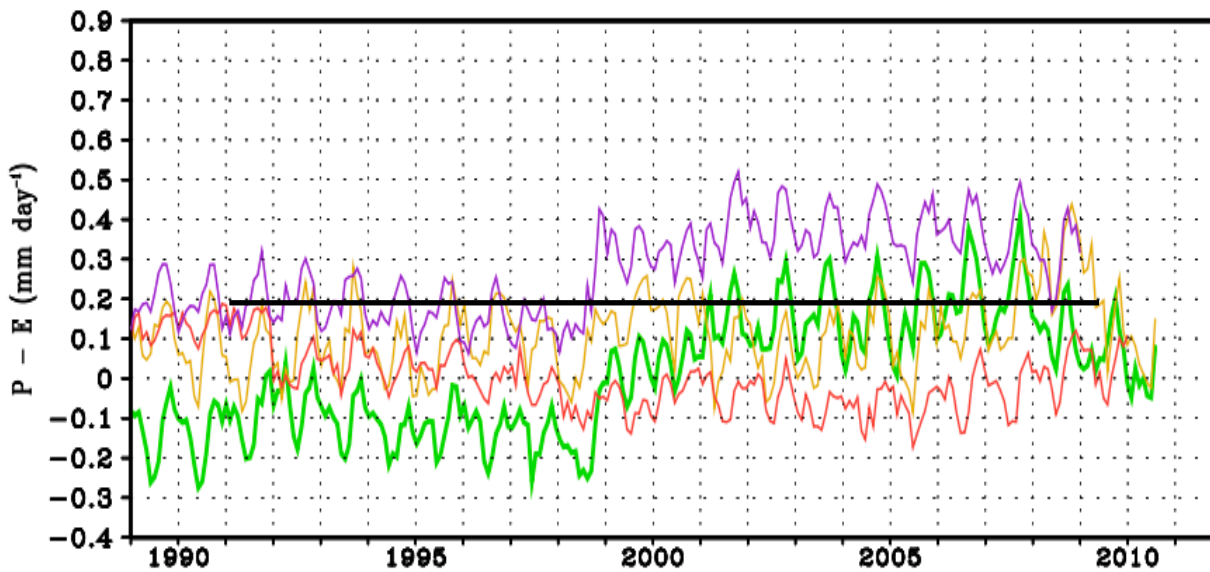


Figure 20b: Global mean analysis increment of moisture inferred from the imbalance between evaporation and precipitation, from ERA-Interim (red), JRA-25 (orange), MERRA (green), and CFSR (purple).

AMSU-A has a strong impact on the annual cycle in MERRA (Figure 21), much more so than in (and in the opposite direction to) CFSR (not shown). 20CR does not show this effect, providing additional evidence of the link to the satellite observing system (Zhang et al., 2012).

On the other hand, substantial progress has been made in representing trends in near-surface air temperature over land (e.g., Figures 22a and 22b), even though surface observations affect the upper-air reanalyses only indirectly via the land-surface boundary conditions used by the forecast model (Simmons et al., 2010).

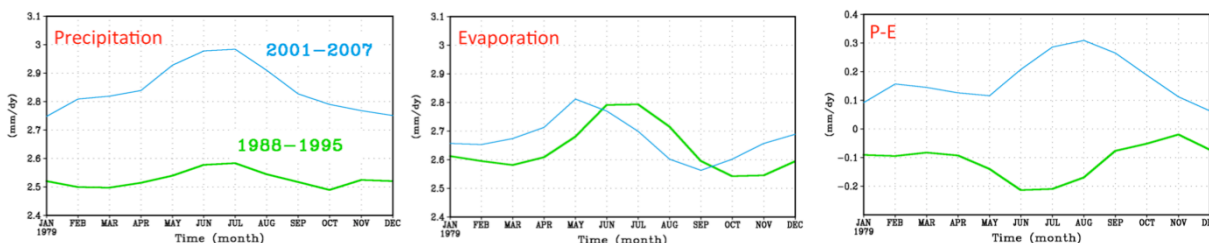


Figure 21: The annual cycle of the global mean precipitation, evaporation, and their difference, from MERRA. The pre-AMSU era is shown in green and the post-AMSU era in cyan.

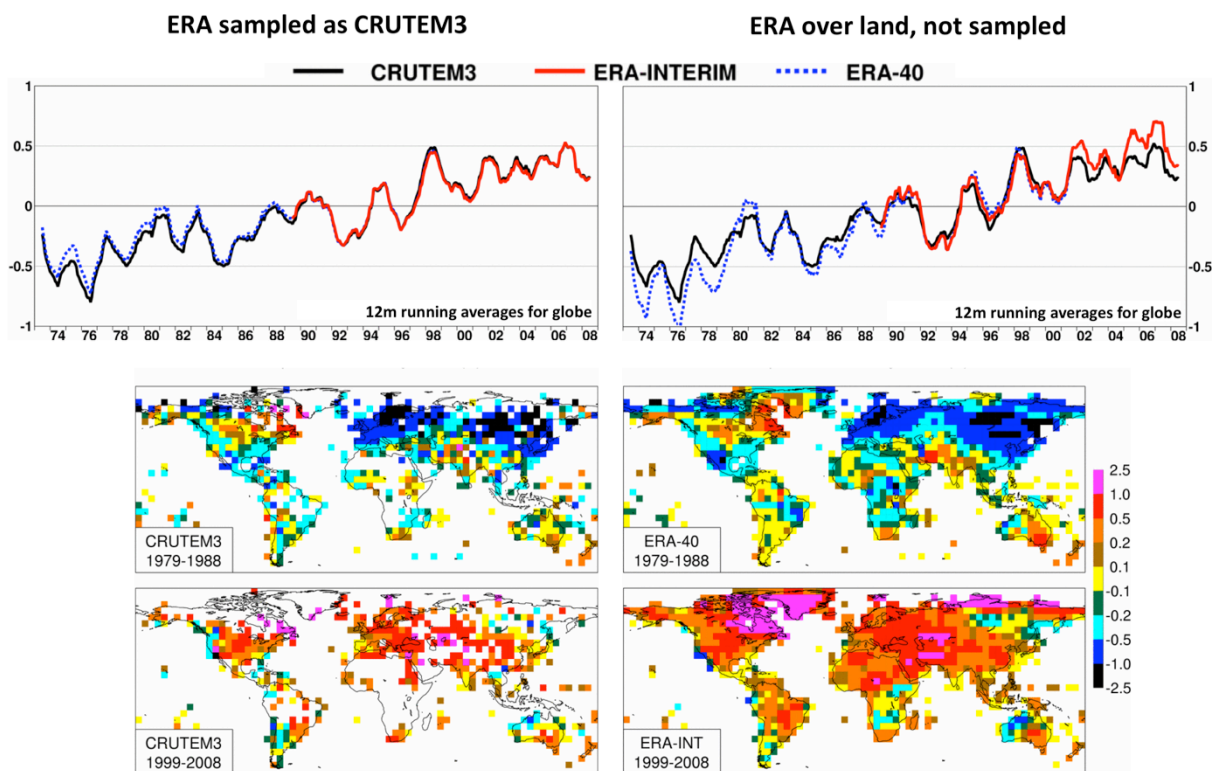


Figure 22a: Temperature anomalies at 2m (K) calculated relative to the 1989-1998 mean. The time series from ERA-40 and ERA-Interim are compared against the CRUTEM3 observations (Brohan et al., 2006). The topmost panels are the time series of 12-month running global average anomalies. The top left-hand panel is the time series from anomalies sampled according to availability of CRUTEM3 data (see lower set of panels); the top right-hand panel is from the raw time series.

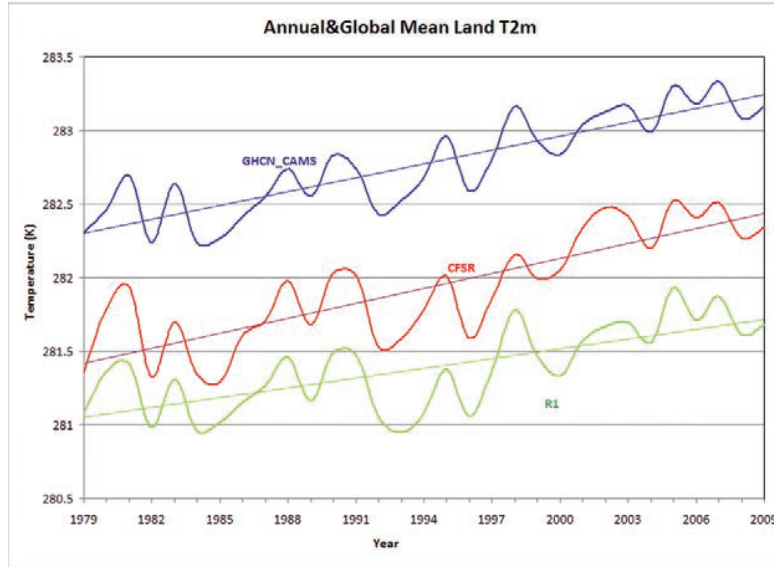


Figure 22b: The annual global mean 2-m temperature over land in NCEP-NCAR R1 (green), CFSR (red), and GHCN-CAMS (blue) over the period of 1979–2009. Units: K. Least squares linear fits of the three time series against time (thin lines). The linear trends are 0.66 , 1.02 , and $0.94 \text{ K (31 yr)}^{-1}$ for R1, CFSR, and GHCN-CAMS, respectively. (Note that straight lines may not portray climate change trends accurately). [From Saha et al. (2010)]

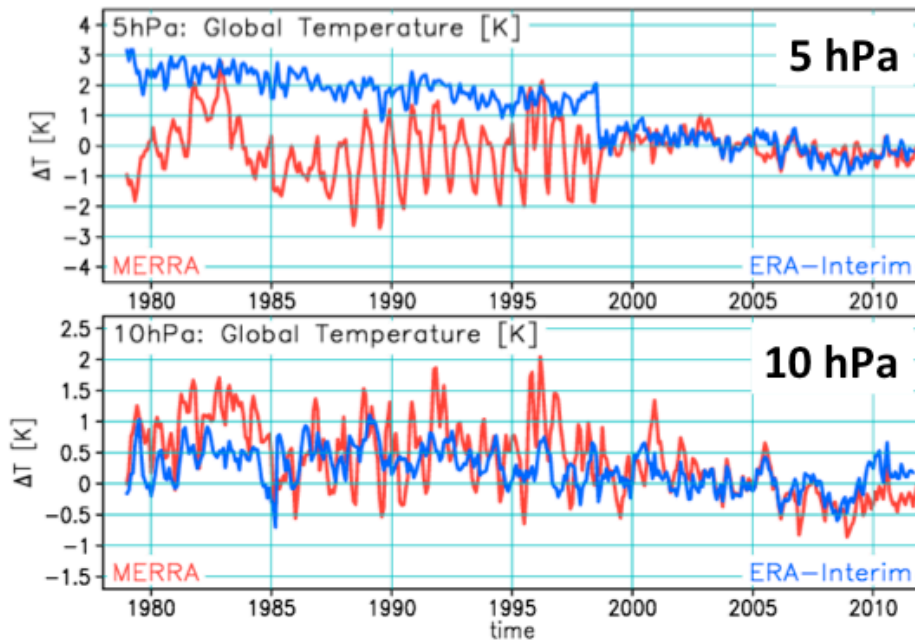


Figure 23: Global mean temperature anomalies (K) in the middle stratosphere from ERA-Interim (blue) and MERRA (red). Data are shown for 5hPa (top) and 10hPa (bottom). The anomalies are computed from the mean annual cycle in 2000–2010 for each individual analysis.

Figure 23 shows time series of the middle stratospheric monthly temperature anomalies in MERRA and ERA-Interim. Anomalies are calculated relative to the mean annual cycle in 2000-2010, a period of relative stability in both time series. ERA-Interim shows a discontinuity at 5 hPa in 1998 with the introduction of AMSU-A. While MERRA does not show an obvious SSU-AMSU transition in 1998, it does show evidence of data instability when the first versions of SSU data were available. In the 1980s when SSU was available on both AM and PM platforms with relatively short lifetimes, the time series has marked interannual variability. With the advent of NOAA-11 and NOAA-14, the time series is more stable, but with large annual cycles. This is a complex issue that needs to be addressed in more detail in future reanalyses: it depends on the presence of model biases, the details of the radiative transfer modeled used, the bias correction, and the lack of information on vertical structure inherent in the nadir observations available for reanalysis. At 10 hPa, where the temperature is more strongly constrained by radiosonde and other data, the variations are more stable and the SSU-AMSU transition is not noticeable. However, the issues associated with SSU in MERRA still leave their imprint.

4. Planning Future Atmospheric Reanalyses

The first generations of reanalyses from NCEP and ECMWF have proven to be extremely valuable scientific tools, enabling climate and weather research not otherwise possible. Their utility stems from the availability of data at regular intervals in time and space, including many variables not directly observed. An important caveat for users, however, is that a reanalysis is not an observation data set, but rather a merged product of model fields constrained by observations. Since the observational constraint is only partial and, moreover, varies in space and time, biases in the model can result in spurious signals in the reanalyzed fields. As such, understanding how errors and uncertainties in both models and observations affect the quality of the reanalysis is crucial for gauging its utility as well as the uncertainty in the reanalysis itself.

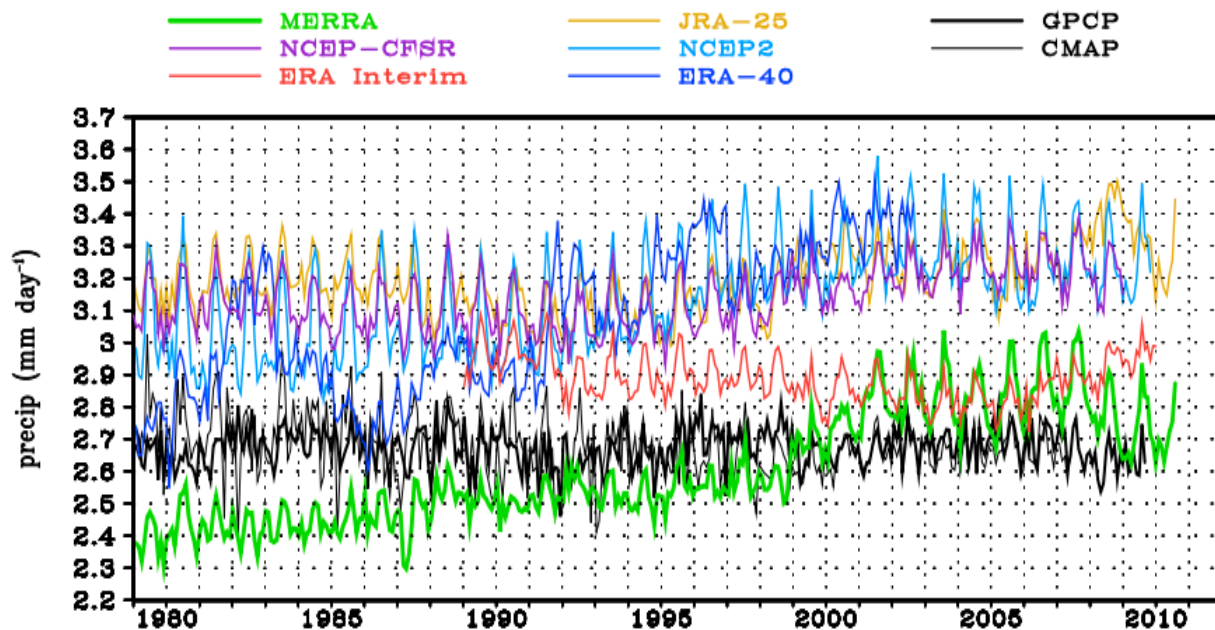


Figure 24: Global mean precipitation (mm day^{-1}) for the available reanalyses compared against two observational data sets, GPCP and CMAP.

Significant improvements have come from each generation of reanalyses. Both the improvements and many of the remaining deficiencies are apparent in the (extended) time series of global mean precipitation shown in Figure 24. Many improvements have come from the NWP imperative, for which the systems will continue to evolve, taking advantage of new data types and improved data assimilation methodologies. However, the question remains as to what needs to be done to improve reanalyses further, especially to address jumps and false trends associated with changes in the observing system.

While agreeing that addressing the issue of artificial trends associated with the changing observing system is a top priority, workshop participants concluded that continuing to update reanalyses is still useful:

- To include improvements in data, using previously unused data (cloudy radiances, etc.)
- To include improvements in models (e.g., reduced biases with resolution)
- As we develop the implementations to help deal with the changing observing system (e.g., changing the background error covariance, \mathbf{B} , with the observing system)
- To provide fields needed for historical re-forecasts for short-term climate
- To make still further major improvements in the water and energy cycle budgets.

The main issues to be addressed for the next generation reanalyses were identified as:

- Improving the hydrological cycle
- Improving the quality of the reanalyses in the stratosphere
- Improving quality of the reanalyses over the polar regions
- Improving estimates of uncertainty
- Reducing spurious trends and jumps
- Extending the reanalysis record for as long as possible, to include the 1970s for reanalyses focused on the satellite era, and to go back at least to 1850 with those reanalyses using sparse observations.

4.1 Model

As seen in Figure 20, the “responses” to observing system changes are very different among the different reanalyses. These responses can depend on the analysis method and/or the model used for data assimilation. What is clear is that correcting model biases will be an important element of reducing both the size of analysis increments and also reducing spurious trends and jumps associated with changes in the input data streams.

4.2 Assimilation System

Accounting for changes in the observing system over time is a major challenge for data assimilation in the context of reanalysis, and one that is likely to increase in significance as reanalyses are extended over many decades, and even centuries. While improved models will likely reduce the (often deleterious) effects of observing system changes on reanalysis quality and consistency, data assimilation systems still must be adapted to reflect these changes in terms of the expected accuracy of the background forecast. For example, it is well known that the quality of an analysis produced with a sparse observing system is highly sensitive to the

specification of the background error covariances. As noted in section 2, ensemble-based data assimilation systems provide a unique capability in this regard. However, since most centers involved in generating the current- (and, presumably, next-) generation reanalyses will likely continue running some form of variational scheme, strategies for adapting the background error covariances in these systems should be considered.

NCEP and GMAO (in collaboration with ESRL) and ECMWF are developing hybrid variational schemes in which the background error covariances are augmented or replaced by information produced by an ensemble system running in some tandem configuration. The potential benefits of such systems for NWP have already been demonstrated (e.g., Buehner et al., 2010a, b), but it remains to be seen whether such schemes are in regular use by the time the next-generation reanalysis are produced. In the meantime, the JMA has begun its JRA-55 reanalysis using a traditional 4D-Var scheme, but with a simple inflation factor applied to the background error variances during the pre-satellite era. Pre-production tests have shown modest, but noticeable, positive impacts with this technique in terms of fits-to-observations, upper-air analysis errors and forecast skill (Ebita et al., 2011).

The effects of model error can also be accounted for (to varying degrees) within the context of the data assimilation scheme. The GMAO has experimented with a variational model bias correction scheme run as part of the minimization—analogue to the variational observation bias correction scheme discussed in section 2—as well as with the application of time-averaged or slowly varying bias estimates (produced by this scheme beforehand) as a forcing term in the model equations (analogue to IAU). Neither approach has produced consistently beneficial results so far, but will likely be re-examined as part of the development effort for the follow-on to MERRA.

Ultimately, a weak-constraint formulation, in which a model error term is added to the analysis cost function, must be employed to produce an optimal analysis. However, specification of the required model error covariance operator (required in the context of 4D-Var) remains a significant stumbling block. ECMWF has experimented with several weak-constraint configurations, representing various levels of approximation to the full four-dimensional problem. A version of weak constraint 4D-Var applied to the stratosphere (without model error cycling) has been running operationally at ECMWF since late 2009 (e.g., Trémolet, 2006) and it is expected that the next reanalysis produced by ECMWF will be run with some form of weak-constraint 4D-Var. The 4D-Var systems under development at GMAO and NCEP are also weak-constraint capable, but have undergone only limited testing to date.

Users of reanalysis data often request a characterization of the quality of and the uncertainty in the fields. While intercomparison with reference data sets is common practice for ascertaining quality, such comparisons are usually restricted to long-term climatological statistics and seldom provide state-dependent measures of the uncertainties involved. The ensemble nature of the 20CR provides a new capability in atmospheric reanalysis: it is the first reanalysis dataset to estimate the uncertainty in the analysis fields at each analysis time, albeit according to the model ensemble used. To evaluate whether the ensemble uncertainty varies as expected with the time-changing observation network, Figure 25 compares the expected error (red curves) to the actual RMS differences of the increments: the first-guess ensemble mean minus the assimilated observations (blue curves). The time variation of the actual and expected error is consistent with

the variations in the number of observations used in the analysis (black curves; note the log scale).

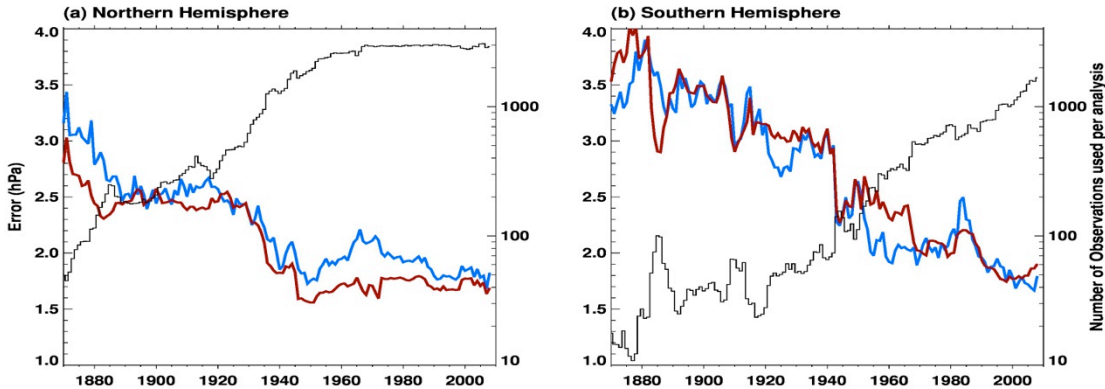


Figure 25: Time series of the 6-hourly first guess (blue curves) root-mean-square (RMS) difference from pressure observations and (red curves) expected RMS difference calculated over separate years from 1870 to 2008 for the (a) northern hemisphere (20°N-90°N) and (b) southern hemisphere (20°S-90°S). The square root is calculated on the annual mean square values. The thin black curve shows the average number of pressure observations for each analysis in the indicated year (note the logarithmic scale). [From Compo et al. (2011)]

Comparison of such estimates with the statistics of differences between the most recent reanalyses using the full observing suite would be a useful undertaking. The innovations and analysis increments provide additional information on the quality of the analyses, as well as on the consistency of the different observations and how they are represented in the analysis. In addition to sharing observations, it would be useful for reanalysis producers to share such information on system performance in order to guide future development. The sharing of these and other metrics as part of future reanalyses would benefit users as well.

4.3 Observations

Just as source codes for models and data assimilation systems are version-controlled so that changes are traceable, so too is it important to track the quality and release history of observational data sets used for reanalysis. The need for this capability is likely to increase as the number and types of available observations increase and as existing data sets are reprocessed to improve their quality and information content. For example, the Global Space-Based Inter-Calibration System (GSICS) has been established in part to retrospectively re-calibrate a wide range of archived satellite data sets to increase their utility for reanalysis and climate studies. Currently, there is no central data steward for reanalysis input observations, but only some informal sharing of observations and quality information between reanalysis centers. All participants in the workshop agreed that some centralization would be beneficial to future reanalyses, and it was noted that the WCRP Observations and Analyses Panel (WOAP) has initiated a committee to address this issue. So as to maximize the cross-center collaborations, participants agreed that future reanalyses should avoid using proprietary observations or input data sets. In the meantime, the current reanalyses have helped identify biases and trends in

currently available satellite and *in situ* data sets that should be addressed in preparing for future reanalyses.

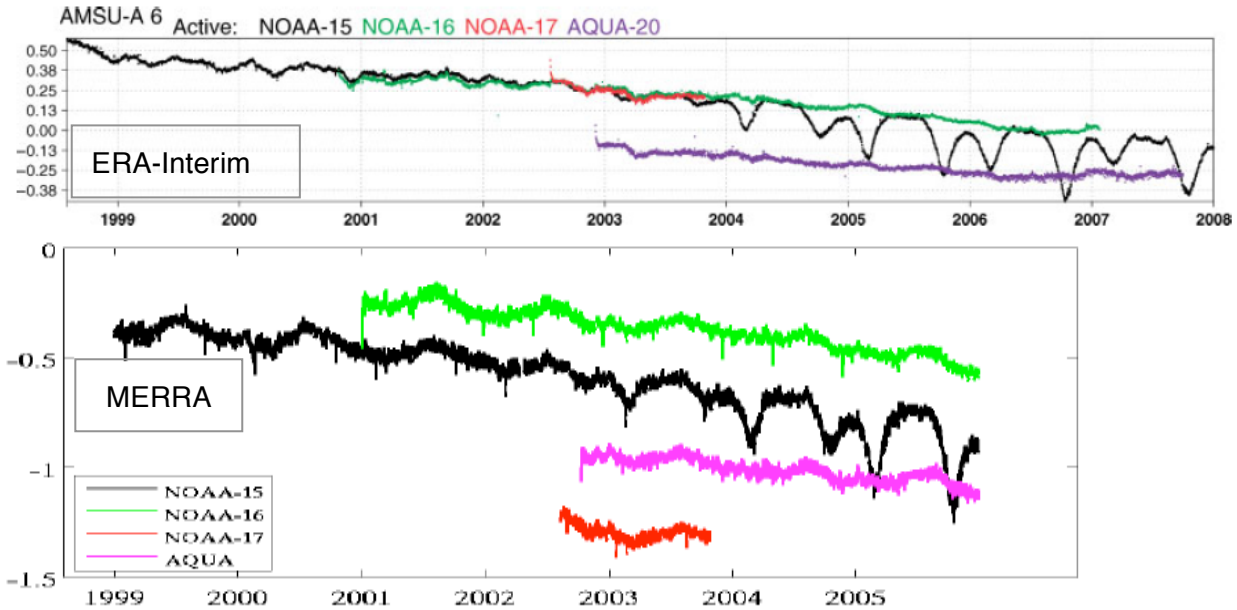


Figure 26: Globally averaged bias estimates (K) for AMSU-A channel 6 radiances from NOAA-15, -16, -17 and Aqua based on ERA-Interim (from Dee and Uppala (2009), top) and MERRA (bottom). The bias estimates based on a 12-hourly assimilation cycle in ERA-Interim and a 6-hourly assimilation cycle in MERRA.

DU09 identified a number of such issues by analyzing the performance of the variational bias correction scheme for satellite radiances used in ERA-Interim. Figure 26 shows results from that paper, indicating a long-term trend in the global bias estimates for AMSU-A channel 6 radiances from different satellites, as well as similar results based on MERRA. Both reanalyses show a downward trend as large as 0.5 K per decade, although the bias estimates themselves differ in each system as a result of the different background states and other observational information. Dee and Uppala attributed this trend to known instrument problems, but also noted that the trends may be over-exaggerated in these results due to the assimilation of increasing numbers of (warmly) biased aircraft observations in the upper troposphere. Evidence of the latter is illustrated in Figure 27, which, like Figure 26, compares results from DU09 for ERA-Interim with ones for MERRA, but in this case showing observation-minus-analysis departures and observation counts for radiosonde reports at 200 hPa. Comparison with the same statistic for aircraft temperatures (not shown) shows that the increase in the magnitude of the upper tropospheric bias with respect to radiosondes starting in the mid- to-late nineties coincides with an increase in aircraft observations, which have a warm bias (Cardinali et al., 2003; Ballish and Kumar, 2008; DU09). As pointed out by DU09, after 1999 the mean analyzed temperatures near these altitudes are increasingly determined by the more numerous aircraft data, especially in the Northern Hemisphere, even though the observation error specified for radiosondes tends to be slightly lower than that specified for aircraft (0.65 K for radiosondes and 0.8 K for most aircraft observations at 300 hPa in MERRA).

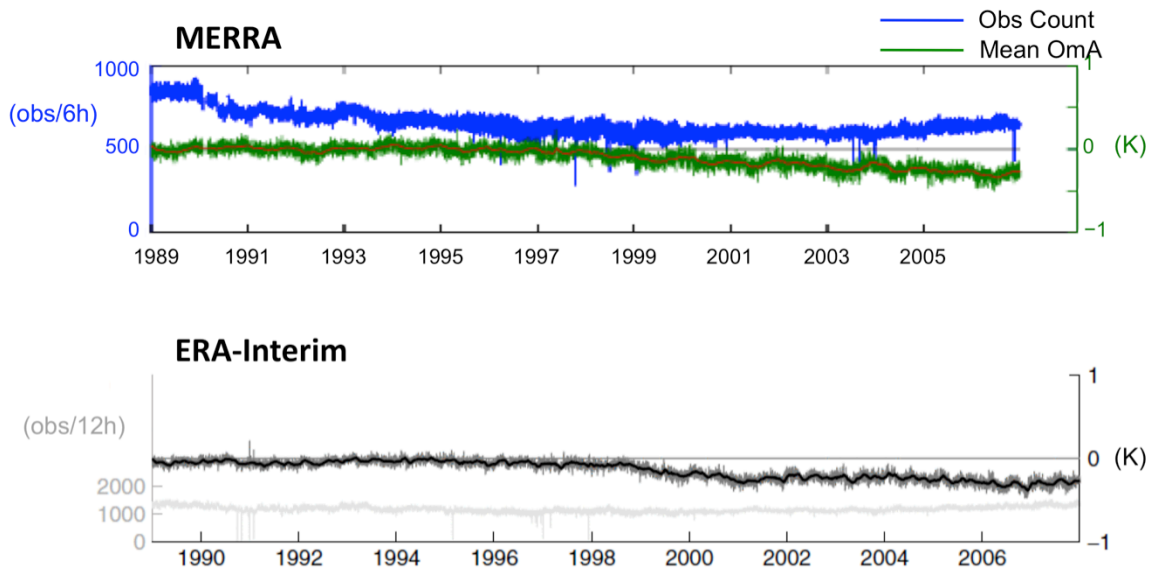


Figure 27: Globally analysis departures (K) and observation counts for radiosonde observations at 200 hPa based on MERRA (top) and ERA-Interim (from Dee and Uppala (2009), bottom). Observation counts represent 12-hour totals in ERA-Interim and 6-hour totals in MERRA.

As noted above, off-line bias corrections (Redder et al., 2004) and a “homogenization” procedure (Haimberger, 2007) have been applied to radiosonde observations in MERRA, and it has been proposed to apply bias corrections to aircraft temperature observations (Balish and Kumar, 2008). There is some effort underway to develop bias adjustments for radiosonde winds and moisture. Bias corrections were made to surface pressure data as part of 20CR. Ultimately, bias corrections for conventional observations are likely best estimated within the data assimilation scheme so as to be adaptive and consistent with all other information used in the analysis.

It is also worth noting here that most centers make only limited use of surface-sensitive radiance data over land or snow- and ice-covered surfaces that might otherwise be important sources of information in a reanalysis context. In MERRA, for example, microwave radiances from AMSU-A channels 1-6 and 15 were excluded over snow, ice and mixed surfaces, as were radiances from AMSU-B channels 1, 2 and 5, and MSU channels 1 and 2. Surface-sensitive infrared radiances were also excluded over land. Successful use of these data requires, amongst other things, improved modeling of surface emissivity and other relevant land surface characteristics.

A number of operational data suppliers have reprocessed some of their products for climate studies and reanalysis purposes. For example, ESA has produced a complete set of ERS-1 and ERS-2 ocean surface winds, 1991-2007. EUMETSAT has reprocessed METEOSAT winds from 1982-1987, with plans to reprocess more. JMA has produced reprocessed GMS winds from 1987 through 2003. The GSICS in conjunction with NESDIS is in the process of recalibrating a number of the historical TOVS radiance datasets. Projects such as these are very important for improving the quality of existing (and future) satellite data sets for reanalysis.

To adequately address the preparation of conventional (non-satellite) data, the problem revolves around a much longer and more scattered archive of observations. For example, there is still the need for discovery and recovery of significant parts of the observed record of the 20th century. Even the satellite era (1979-present) conventional datasets are still to some degree fragmented among national, military, university, and other sources, although overall the situation has been greatly improved under the auspices of preparation for reanalysis projects completed so far. Due in part to the ongoing success of reanalysis efforts, there has been growing movement within traditional climate data centers such as NCDC and NCAR to consolidate their disparate archives and produce standardized and combined “macro” datasets suitable for reanalysis input. This very welcome development constitutes a big step towards some centralization of the stewardship of reanalysis data. These centers have the mandate and wherewithal to document observations’ provenance across versions of the datasets, and possibly including records of observation performance in different reanalysis projects. Several independent initiatives to recover and modernize historical observation from diverse sources, such as the ACRE project (Allan et al., 2011) and the International Surface Temperature Initiative (Thorne et al. 2011), are also very productive overlaps between strictly climate research interests and NWP/reanalysis attempts to recreate climate from observations.

Another major observational issue is the lack of long-term *in situ* temperature observations of the upper stratosphere, which, coupled with the model biases and the deep weighting functions of the SSU and AMSU-A radiance channels, makes precise constraints on meteorological fields rather difficult to ascertain. It also makes stratospheric satellite bias corrections difficult because of the major contributions of model bias in variational bias correction techniques. Figure 23 illustrates long-term temperature fluctuations that exceed the magnitude of expected decadal trends. Obviously, future reanalyses will need to focus on improving models (eliminating model biases) and also better calibrations of the input radiance data and improvement in the way these interact with the background states to produce the analyses.

Limb-sounding temperature data are available for certain periods, and may be used as “anchors” for limited numbers of years, but these datasets generally do not overlap, so issues related to cross-dataset bias have not been addressed in detail. High-quality temperature time series are available from occultation measurements, but the extremely low density of these data makes them less useful for assimilation: a more promising way of use in reanalyses might be as calibration datasets – an aspect that will require substantial developments. The CFSR used reprocessed CHAMP and COSMIC occultation data starting in 2001, but these data are still more or less experimental, and a work in progress.

Similar arguments apply to ozone analyses, for which the SBUV data provide generally adequate constraints at any time, but issues of cross-calibration of the sensors, due to orbital differences and instrument characteristics, need to be addressed. Here, too, the use of sparse occultation observations for calibration may be promising. Additionally, inclusion of time-dependent greenhouse gases and ozone chemistry in the underlying model will be needed to more realistically represent long-term trends in temperature and ozone in the middle atmosphere.

4.4 Anticipated Developments in Coupling to Other Components

4.4.1 Upper ocean and land surface

Many of the questions to be addressed through reanalyses (budgets and exchanges, trends, attribution of major anomalies, etc.) would benefit from consistent analyses across components. Hence there is considerable interest in *integrated Earth System analyses*. The NCEP CFSR is the first atmospheric reanalysis conducted where the first guess was provided by the integration of a coupled ocean-atmosphere-sea-ice-land-surface model. An example of the benefit from coupling can be seen in the correlation between precipitation and SST, compared to earlier reanalyses, seen in Figure 9. It is expected that future developments will have some focus on coupling, whether weakly coupled as in the CSFR or strongly coupled when observations in one component will impact the state in another.

4.4.2 Carbon, aerosols, other constituents

The increased interest in “Earth System” reanalyses that include atmospheric composition is based partly on the widespread use of reanalyses for driving atmospheric aerosol, chemistry and carbon models, and also on the increasing availability of observations of atmospheric composition in the past decade. It is reasonable to work towards reanalyses that include atmospheric aerosols, carbon species, and reactive gases, at least for the post-2000 period, as future projects are formulated. Such Earth System components depend fundamentally on the adequacy of the underlying meteorological analyses to constrain aspects such as transport (winds), reactive chemistry (temperature), and emissions of numerous constituents that depend variously upon physical properties such as surface winds (e.g., sea salt, dust, oceanic carbon exchange), surface temperature (e.g., isoprene), soil moisture (CO₂). Additional constraints from space-borne sensors can be included into these analyses, such as leaf-area index (e.g., MODIS) that helps constrain respiration and photosynthesis calculations, burned areas and fire radiant energy (e.g., MODIS) that helps constrain CO, CO₂, black- and organic-carbon aerosol emissions, and additional chemical species, such as NO₂ (e.g., from OMI and GOME), that help constrain air pollution. Inclusion of these additional observations to variously constrain emissions and chemical processes adds complexity to the underlying models used in reanalyses, transporting additional species and computing the interactions among them, and adds additional cost to the analyses (more variables in the state vectors).

While assimilation of these constituents is in theory straightforward, there are presently many uncertainties in the details, such as how to best represent background error covariances (with potential cross-species components and co-variance with temperature and transport). It is also important to realize that the multi-decadal analyses that the community has come to expect for meteorology are highly unlikely to be performed for a broad range of aerosols and constituents because of the dearth of relevant observations over the past decades.

5. Cross-Center Coordination for the Next-generation Reanalyses

The workshop participants agreed that to improve the representation of the climate record in reanalyses it will be necessary to understand some of the sensitivities and responses of the assimilation systems to the different input data as well as the impact of different input data (such as the use of cross-calibrated MSU vs. using the variational bias correction to account for MSU channel drifts).

An obvious area that needs investigation is the sensitivity of the different systems to the introduction (and removal) of the AMSU-A instruments on NOAA-15 and -16. Each system responds differently, but there is an imprint of change in global precipitation in many of the systems (Figure 20). Differences may reflect differences in QC measures. For example, developers at NCEP and GMAO cited a potential deficiency in QC for the water vapor sensitive channels (1-5 and 15) on AMSU-A in the GSI used for MERRA as compared to ERA-Interim. Hence the suggestion followed to undertake an in-depth investigation of how these channels were used in the various reanalyses. Another difference between the systems is the assimilation of rain-affected radiances (1d+4d var) in ERA-Interim. This was implemented/modified in ERA-Interim in 1992 and had a noticeable impact on the global precipitation (Figure 20a). This then may lessen the impact of new data on the global precipitation in the ERA-Interim system. Obviously judicious experimentation and comparison may provide insight into the variations that are of concern.

The groups agreed to start a joint project of sensitivity analysis:

- Examine data utilization, including QC decisions and innovation statistics
- Identify joint experiments to be conducted to elucidate common issues
- Share information on results from sensitivity experiments.

To set the stage for future coordination, reanalysis centers are encouraged to prepare and share lists of anomalous behavior or features to help identify how common such anomalies are across the various reanalyses.

5.1 Observations

Much of the hard work in developing reanalyses is the assembly and processing (including correction and QC) of the observations. Crucial new inputs, including updated versions of the International Comprehensive Ocean Atmosphere Data Set (Worley et al., 2005) and the International Best Track Archive for Climate Stewardship (Knapp et al., 2010), millions of newly recovered surface observations (Yin et al., 2008), and improved satellite records (e.g., Zou et al., 2006), were important contributions to the improvement of the current reanalyses over the previous generation. A workshop on improving observations for reanalysis (Schubert et al., 2006) recommended improvements to historical observations (including data mining), improved quality control, and further cross-calibration and bias-correction of observations to help to reduce the impacts from changes in the observing system. As noted above, some centralization and coordination on input observations and ancillary data would be beneficial to future reanalyses. One recommendation was for ACRE to expand from contributing surface observations to just the 20CR to contributing to all future reanalysis efforts, possibly acting as a data coordinator and provider of surface data for all future reanalyses in collaboration with working groups of GCOS and WCRP.

5.2 Innovative Diagnostics

Given the lack of definitive validation data and the vast array of possible comparisons, the workshop participants encouraged the development of innovative diagnostics. Some examples:

- A useful metric of both quality and uncertainty is the level of variance of one reanalysis explained by another. This should be a standard diagnostic for the various reanalyses.
- Summaries such as the joint frequency distribution of long-wave and short-wave fluxes in Figure 7, developed by J. Chen, provide a new and efficient view of the quality of the radiative analyses.
- A contextual bias analysis, as developed by A. da Silva, helps to see if different types of observations are providing conflicting information to the analysis.

The workshop participants also proposed the identification of important metrics to assess reanalysis quality, beyond NWP skill.

5.3 Standard Intercomparisons and Benchmarks Including Community Involvement

The participants agreed that a mechanism for the timely exchange of information about the quality of the reanalyses, results of experiments, and plans for future developments was needed. As a response to this recommendation, the Reanalysis Intercomparison and Observations collaborative wiki site at Reanalyses.org was formed with support from NOAA, GCOS, WCRP, and ACRE and the active participation of all of the centers generating the datasets. At NOAA's request, the site was expanded to include ocean reanalyses. The goal of Reanalyses.org is to facilitate comparison between reanalysis and observational datasets. Evaluative content provided by reanalysis developers, observationalists, and users; and links to detailed data descriptions, data access methods, analysis and plotting tools, and dataset references are available. One focus is on discussions of the recovery of observations to improve reanalyses. The wiki framework encourages scientific discussion between members of Reanalyses.org and other reanalysis users.

5.4 Coordinating Ancillary Products: Accessible Assimilated Observations and Statistics

Making progress in understanding the (possibly different) sensitivities of the different systems to changes in the observing system, or (for example) identifying any benefits from prior cross-calibration of different satellites, will take a concerted effort at comparing information in the ancillary “feedback data” generated through the process of assimilation: innovations, bias corrections, outcomes of data selection algorithms, cloud detection outcomes, etc. In addition, examination of gridded feedback files and contextual bias analyses should be helpful to understand how the data are impacting the system performance. Initial progress in making these feedback data available has been made. For the 20CR, the feedback data are available from the International Surface Pressure Databank (rda.ucar.edu/datasets/ds132.0). The gridded feedback files from MERRA are available online with the primary MERRA products at <http://disc.sci.gsfc.nasa.gov/mdisc/>.

5.5 Moving Forward

Workshop participants agreed to identify a small group to coordinate these efforts between the centers. Support or organization of such coordination at the international level would facilitate collaborations at the technical level and ensure advances for the next generation of reanalyses. Participants agreed that resources directed to operational and laboratory development of

reanalyses was crucial for future success and continued improvement of these vital datasets. This is consistent with the action item C12 in the 2010 GCOS Implementation Plan (GCOS, 2010). University research will also be an important component of developing advances for the next generation of reanalyses.

6. Summary of Recommendations

Target areas for improvements for the next generation of atmospheric reanalyses include:

- The hydrological cycle
- The quality of the reanalyses in the stratosphere
- The quality of the reanalyses over the polar regions
- Representation of surface fluxes
- Observational bias corrections and/or cross-calibration across platforms
- Estimates of uncertainty in the analyses, and
- Reductions of spurious trends and jumps associated with the changing observing system.

Several recommendations were made regarding areas for coordination between reanalysis centers in order to prepare for the next reanalyses:

- Preparation and sharing of lists of anomalous behavior or features to help identify how common anomalies are across the various reanalyses.
- Examination of data utilization, including QC decisions, innovation statistics, bias corrections, outcomes of data selection algorithms, cloud detection outcomes, etc.
- Identification of joint experiments to be conducted to elucidate issues found to be in common in different reanalyses.
- Sharing of results from jointly designed sensitivity experiments.
- Coordination of input observations and ancillary data and centralization of the serving of these observations where possible.
- Expansion of ACRE's efforts for contributing surface observations to 20CR to contributing to all future reanalysis efforts, possibly acting as a data coordinator and provider of surface data for all future reanalyses in collaboration with working groups of GCOS and WCRP.
- Development of innovative diagnostics and metrics to help quantify observational issues, the quality and also agreement of the reanalyses.

The workshop recommended that a mechanism be established for the timely exchange of information about the quality of the reanalyses, results of experiments, and plans for future developments. This idea was quickly embraced with the establishment of **Reanalysis.org**. However, further progress is needed in the utilization of such a capability to enhance communications between reanalysis groups.

Finally, consistent with the Arkin et al. (2003) workshop report, the workshop participants recommended extending the reanalysis record for as long as possible, to include the 1970s for

reanalyses focused on the satellite era, and to go back at least to 1850 with those reanalyses using sparse observations.

7. References

- Allan, R., P. Brohan, G.P. Compo, R. Stone, J. Luterbacher, and S. Brönnimann, 2011: The International Atmospheric Circulation Reconstructions over the Earth (ACRE) initiative. *Bull. Amer. Meteor. Soc.*, **92**, 1421-1425. doi: 10.1175/2011BAMS3218.1.
- Anderson, J.L., B. Wyman, S. Zhang, and T. Hoar, 2005: Assimilation of surface pressure observations using an ensemble filter in an idealized global atmospheric prediction system. *J. Atmos. Sci.*, **62**, 2925-2938.
- Arkin, P, E. Kalnay, J. Laver, S. Schubert, and K. Trenberth, 2003: Ongoing Analysis of the Climate System: A Workshop Report. Boulder, CO., August 18-20, 2003. Available at http://www.joss.ucar.edu/joss_psg/meetings/archived/climatesystem/FinalWorkshopReport.pdf
- Ballish, B. A., and V.K. Kumar, 2008: Systematic differences in aircraft and radiosonde temperatures. Implications for NWP and climate studies. *Bull. Amer. Meteor. Soc.*, **89**, 1689-1707.
- Berrisford P., D.P. Dee, K. Fielding, M. Fuente, P. Kållberg, S. Kobayashi, and S.M. Uppala, 2009: The ERA-Interim Archive. *ERA Report Series, No.1*. ECMWF: Reading, UK.
- Bosilovich, M., J. Chen, F.R. Robertson and R.F. Adler, 2008: Evaluation of Global Precipitation in Reanalyses. *J. Appl. Meteorol. Climatol.*, **47**, 2279–2299.
- Brohan, P., J.J. Kennedy, I. Harris, S.F.B. Tett and P.D. Jones, 2006: Uncertainty estimates in regional and global observed temperature changes: a new dataset from 1850. *J. Geophys. Res.*, **111**, D12106, doi:10.1029/2005JD006548.
- Buehner, M., P.L. Houtekamer, C. Charette, H. L. Mitchell, and B. He, 2010a: Intercomparison of Variational Data Assimilation and the Ensemble Kalman Filter for Global Deterministic NWP. Part I: Description and Single-Observation Experiments. *Mon. Wea. Rev.*, **138**, 1550-1566.
- Buehner, M., P.L. Houtekamer, C. Charette, H. L. Mitchell, and B. He, 2010b: Intercomparison of Variational Data Assimilation and the Ensemble Kalman Filter for Global Deterministic NWP. Part II: One-month experiments with real observations. *Mon. Wea. Rev.*, **138**, 1567–1586.
- Cardinali C., L. Isaksen, and E. Anderson, 2003: Use and impact of automated aircraft data in a global 4DVAR data assimilation system. *Mon. Wea. Rev.* **131**: 1865–1877.
- CCSP, 2008: Reanalysis of Historical Climate Data for Key Atmospheric Features: Implications for Attribution of Causes of Observed Change. A Report by the U.S. Climate Change Science Program and the Subcommittee on Global Change Research [Randall Dole, Martin Hoerling, and Siegfried Schubert (eds.)]. National Oceanic and Atmospheric Administration, National Climatic Data Center, Asheville, NC, 156 pp.

- Compo, G.P., J.S. Whitaker, and P.D. Sardeshmukh, 2006: Feasibility of a 100-year reanalysis using only surface pressure data. *Bull. Am. Met. Soc.*, **87**, 175-190, doi: 10.1175/BAMS-87-2-175.
- Compo, G.P., and Coauthors, 2011: The Twentieth Century Reanalysis Project. *Q. J. Roy. Meteorol. Soc.* **137**, 1-28.
- Dee, D.P., and S. Uppala, 2009: Variational bias correction of satellite radiance data in the ERA-Interim reanalysis. *Q. J. Roy. Meteorol. Soc.*, **135**, 1830–1841.
- Dee, D.P., and Coauthors, 2011a: The ERA-Interim reanalysis: Configuration and performance of the data assimilation system. *Q. J. Roy. Meteorol. Soc.*, **137**, 553-597.
- Dee, D., P. Poli, and A.J. Simmons, 2011b: Extension of the ERA-Interim reanalysis to 1979. *ECMWF Newsletter No 128*, Summer 2011, p.7.
- Derber, J. C., and W.S. Wu, 1998: The Use of TOVS Cloud-Cleared Radiances in the NCEP SSI Analysis System. *Mon. Wea. Rev.*, **126**, 2287–2299.
- Douglass, A.R., C.J. Weaver, R.B. Rood, and L. Coy, 1996: A three-dimensional simulation of the ozone annual cycle using winds from a data assimilation system, *J. Geophys. Res.*, **101**, 1463-1474, doi: 10.1029/95JD02601.
- Ebita, A., and co-authors, 2011: The Japanese 55-year Reanalysis “JRA-55”, 2011: An Interim Report, *SOLA*, **7**, 149-152, doi: 10.2151/sola.2011-038.
- Gaspari, G., S.E. Cohn, J. Guo, and S. Pawson, 2006: Construction and Application of Covariance Functions with Variable Length Fields. *Q. J. Roy. Meteorol. Soc.*, **132**, 1815-1838.
- GCOS, 2010: Implementation Plan for the Global Observing System for Climate in Support of the UNFCCC (2010 Update). GCOS-138 (WMO-TD/No. 1523), August 2010. <http://www.wmo.int/pages/prog/gcos/Publications/gcos-138.pdf>.
- Geer, A.J., P. Bauer, and P. Lopez, 2008: Lessons learnt from the operational 1D+4D-Var of rain- and cloud-affected SSM/I observations at ECMWF. *Q. J. Roy. Meteorol. Soc.*, **134**, 1513-1525.
- Haimberger, L., 2007: Homogenization of radiosonde temperature time series using innovation statistics. *J. Climate*, **20**, 1377-1403.
- Haimberger, L., C. Tavolato, and S. Sperka, 2008: Toward elimination of the warm bias in historic radiosonde temperature records—Some new results from a comprehensive intercomparison of upper-air data. *J. Climate*, **21**, 4587-4606.
- Kalnay, E., and Coauthors, 1996: The NCEP/NCAR 40-Year Reanalysis Project. *Bull. Amer. Meteor. Soc.*, **77**, 437–471.
- Kanamitsu, M., and co-authors 2002: NCEP–DOE AMIP-II Reanalysis (R-2). *Bull. Amer. Meteor. Soc.*, **83**, 1631–1643.
- Kistler, R., and Coauthors, 2001: The NCEP–NCAR 50–Year Reanalysis: Monthly means CD–ROM and documentation. *Bull. Amer. Meteor. Soc.*, **82**, 247–267.
- Knapp K.R., M.C. Kruk, D.H. Levinson, H.J. Diamond, and C.J. Neumann, 2010: The International Best Track Archive for Climate Stewardship (IBTrACS): Unifying tropical

- cyclone best track data. *Bull. Amer. Meteorol. Soc.*, **91**, 363–376. doi: 10.1175/2009BAMS2755.1.
- Manney, G.L., and co-authors, 2008: The Evolution of the Stratopause During the 2006 Major Warming: Satellite data and Assimilated Meteorological Analyses. *J. Geophys. Res.*, **113**, D11115, doi: 10.1029/2007JD009097.
- Monge-Sanz, B.M., M.P. Chipperfield, A.J. Simmons, and S.M. Uppala, 2007: Mean age of air and transport in a CTM: Comparison of different ECMWF analyses, *Geophys. Res. Lett.*, **34**, doi:10.1029/2006GL028515.
- Onogi, K., and co-authors, 2007: The JRA-25 Reanalysis. *J. Meteor. Soc. Japan*, **85**, 369-432. doi: 10.2151/jmsj.85.369.
- Pawson, S. and M. Fiorino, 1998: The Tropical Lower Stratosphere in Atmospheric Reanalyses. Part 1: Thermal Structure and the Annual Cycle. *Clim. Dyn.*, **14**, 631-644.
- Pawson, S. and M. Fiorino, 1998: The Tropical Lower Stratosphere in Atmospheric Reanalyses. Part 2: The Quasi-Biennial Oscillation. *Clim. Dyn.*, **14**, 645-658.
- Pawson, S., I. Stajner, S.R. Kawa, H. Hayashi, W. Tan, J.E. Nielsen, Z. Zhu, L.-P. Chang, and N.J. Livesey, 2007: Stratospheric Transport Using Six-Hour Averaged Winds from a Data Assimilation System. *J. Geophys. Res.* **112**, D23103, doi:10.1029/2006JD007673.
- Rayner, N.A., D.E. Parker, E.B. Horton, C.K. Folland, L.V. Alexander, D.P. Rowell, E.C. Kent, and A. Kaplan, 2003: Global analyses of sea surface temperature, sea ice, and night marine air temperature since the late nineteenth century. *J. Geophys. Res.*, **108**, doi:10.1029/2002JD002670.
- Redder, C.R., J.K. Luers, and R.E. Eskridge, 2004: Unexplained discontinuity in the U.S. radiosonde temperature data. Part II: Stratosphere. *J. Atmos. Oceanic Technol.*, **21**, 1133–1144.
- Rienecker, M.M., and co-authors, 2011. MERRA - NASA's Modern-Era Retrospective Analysis for Research and Applications. *J. Climate*, **24**, 3624-3648, doi: 10.1175/JCLI-D-11-00015.1.
- Saha, S., and co-authors 2010: The NCEP Climate Forecast System Reanalysis. *Bull. Amer. Meteor. Soc.*, **91**, 1015-1057.
- Schoeberl, M.R., A.R. Douglass, Z. Zhu, and S. Pawson, 2003: A Comparison of the Lower Stratospheric Age Spectra Derived from a General Circulation Model and Two Data Assimilation Systems. *J. Geophys. Res.*, **108**, DOI 10.1029/2002jd002652.
- Schubert, S., D. Dee, S. Uppala, J. Woollen, J. Bates, and S. Worley, 2006: Report of the Workshop on “The Development of Improved Observational Datasets for Reanalysis: Lessons Learned and Future Directions”. University of Maryland Conference Center, College Park, MD, 28-29 September 2005, 31 pp. Available at <http://gmao.gsfc.nasa.gov/pubs/docs/Schubert273.pdf>.
- Simmons, A. J., K.M. Willett, P.D. Jones, P.W. Thorne, and D.P. Dee, 2010: Low-Frequency Variations in Surface Atmospheric Humidity, Temperature, and Precipitation: Inferences From Reanalyses and Monthly Gridded Observational Data Sets. *J. Geophys. Res.*, **115**, 1–21. doi:10.1029/2009JD012442.

- Tan, W., M.A. Geller, S. Pawson, and A.M. da Silva, 2004: A Case Study of Excessive Subtropical Transport in the Stratosphere of a Data Assimilation System. *J. Geophys. Res.*, **109**, D11102 doi:10.1029/2003jd004057.
- Thorne, P.W., and co-authors, 2011: Guiding the creation of a Comprehensive Surface Temperature Resource for 21st Century Climate Science. *Bull. Amer. Met. Soc.*, **92**, ES40–ES47, doi: 10.1175/2011BAMS3124.1.
- Trenberth, K., J.T. Fasullo, and J. Kiehl, 2009: Earth’s Global Energy Budget. *Bull. Amer. Meteorol. Soc.*, **90**, 311-323.
- Trenberth, K.E., J.T. Fasullo, and J. Mackaro, 2011: Atmospheric moisture transports from ocean to land and global energy flows in reanalyses. *J. Climate*, **24**, 4907-4924. doi: 10.1175/2011JCLI4171.1.
- Trémolet, Y, 2006: Accounting for an imperfect model in 4D-Var. *Q. J. Roy. Meteorol. Soc.*, **132**, 2483-2504.
- Wheeler, M. and G.N. Kiladis, 1999: Convectively coupled Equatorial Waves: Analysis of clouds and temperature in the wavenumber–frequency domain. *J. Atmos. Sci.*, **56**, 374-399.
- Whitaker, J.S., and T.M. Hamill, 2002: Ensemble data assimilation without perturbed observations. *Mon. Wea. Rev.*, **130**, 1913–1924.
- Whitaker, J.S., G.P. Compo, X. Wei and T.M. Hamill, 2004: Reanalysis without radiosondes using ensemble data assimilation. *Mon. Wea. Rev.*, **132**, 1190–1200.
- Whitaker, J.S., G.P. Compo, and J.-N. Thepaut, 2009: A comparison of variational and ensemble-based data assimilation systems for reanalysis of sparse observations. *Mon. Wea. Rev.*, **137**, 1991-1999.
- Worley S.J., S.D. Woodruff, R.W. Reynolds, S.J. Lubker, and N. Lott, 2005: ICOADS release 2.1 data and products. *Int. J. Climatol.* **25**, 823–842. DOI: 10.1002/joc.1166.
- Yin X., B.E. Gleason, G.P. Compo, N. Matsui, and R.S. Vose, 2008: The International Surface Pressure Databank (ISPD) land component version 2.2. National Climatic Data Center, Asheville, NC. Available from ftp://ftp.ncdc.noaa.gov/pub/data/ispd/doc/ISPD2_2.pdf.
- Zhang, L., A. Kumar, and W. Wang, 2012: Influence of changes in observations on precipitation: A case study for the Climate Forecast System Reanalysis (CFSR), *J. Geophys. Res.*, **117**, D08105, doi:10.1029/2011JD017347.
- Zou, C., M.D. Goldberg, Z. Cheng, N.C. Grody, J.T. Sullivan, C. Cao, and D. Tarpley, 2006: Recalibration of microwave sounding unit for climate studies using simultaneous nadir overpasses. *J. Geophys. Res.*, **111**, D19114, doi:10.1029/2005JD006798.

Appendix A: Summary of Recent and Ongoing Reanalyses

A.1 NASA MERRA

The development of the Modern-Era Retrospective analysis for Research and Application (MERRA) began with two primary objectives. It was recognized that various aspects of the hydrologic cycle represented in previous generations of reanalyses were not sufficient for climate and weather study, and MERRA proposed to improve upon the water cycle as a contribution to the science community and reanalysis research. MERRA's assimilation of the complete satellite era is intended to place observations from NASA's Earth Observing System satellites in a climate context.

MERRA is based on the GEOS-5 atmospheric data assimilation system, version 5.2.0. The NCEP-GMAO Gridpoint Statistical Interpolation (GSI) analysis is integrated with the GEOS-5 atmospheric model in a six-hour assimilation cycle. At $\frac{1}{2}^\circ$ latitude \times $\frac{2}{3}^\circ$ longitude with 72 vertical levels to 0.01 hPa, the spatial resolution of MERRA is finer than previous generation atmospheric reanalyses. MERRA utilizes Incremental Analysis Updates (IAU) that allows for reduced "spin-down" effects by applying the analysis as a tendency term in the governing equations. The observational forcing on the data from the increments is tallied in the output budgets of the model (e.g. water and enthalpy). MERRA provides complete atmospheric budgets that balance, including the analysis terms.

MERRA was processed in three separate streams, each spun-up in two stages: from a two-year analysis at $2^\circ \times 2.5^\circ$ and then a 1-year analysis on the MERRA grid. Streams 1 and 2 were each extended to overlap the next stream to examine the nature of the spin-up as well as predictability/uncertainty. The final MERRA distribution is from the longer streams 1 and 2, so that the distributed streams 2 and 3 have been spun up for 5 and 4 years, respectively, at MERRA resolution.

The MERRA observational suite was based in good part on the observational processing by NCEP. Notable differences include the ERA surface winds, where an older version was used for MERRA, and the SSM/I input data, which came from Goddard (precipitation) and from RSS (radiances and surface winds). The radiosonde data were processed differently (more similar to ERA-Interim processing) and the ERA-40 blacklist was used.

MERRA product collections are available at the Goddard Earth Sciences Data and Information Services Center (GES DISC, <http://disc.sci.gsfc.nasa.gov/mdisc/>).

A.2 ECMWF ERA-Interim

ERA-Interim (Dee et al., 2011a) is the latest global atmospheric reanalysis produced by the European Centre for Medium-Range Weather Forecasts (ECMWF). The ERA-Interim project was conducted in part to prepare for a new atmospheric reanalysis to replace ERA-40, which will extend back to the early part of the twentieth century. Since the meeting took place, the ERA-Interim reanalysis has been extended backward to include the years 1979 – 1988 (Dee et al., 2011b), so the reanalysis extends from 1 January 1979 to the present, continuing forward in near-real time. Production was accomplished in two streams, from 1979 to 1988 and 1989 onwards. ERA-Interim uses a sequential 4D-Var data assimilation scheme, advancing forward in time using 12-hourly analysis cycles. It is based on IFS release Cy31r2, used for operational

forecasting at ECMWF from 12 December 2006 until 5 June 2007. The model has a spectral T255 horizontal resolution and 60 model layers with the top of the atmosphere located at 0.1 hPa. Since ERA-40, there have been major updates to the model's moist physics components and the assimilation includes rain-affected SSM/I radiances as described in detail by Dee et al. (2011).

Gridded data products include a large variety of 3-hourly surface parameters, describing weather as well as ocean-wave and land-surface conditions, and 6-hourly upper-air parameters covering the troposphere and stratosphere. Vertical integrals of atmospheric fluxes, monthly averages for many of the parameters, and other derived fields have also been produced (Berrisford et al., 2009).

A.3 NCEP CFSR

NCEP has now completed the CFSR for the 31-yr period of 1979–2009. It took almost 2 years to accomplish this feat. The primary improvements, compared to previous NCEP global reanalyses are i) the coupling to the ocean during the generation of the 6-h guess field, ii) an interactive sea ice model, and iii) the assimilation of satellite radiances for the entire period. In addition, the much higher horizontal and vertical resolution (T382L64) of the atmosphere, model, and assimilation improvements over the last 10–15 years, and the use of prescribed CO₂ concentrations as a function of time, make for substantial improvements over R1 and R2, which were run at T62L28 resolution.

Another major advance was the real-time monitoring that took place during the execution of the CFSR. Thousands of graphical plots were generated automatically at the end of each reanalyzed month and were displayed on the CFSR Web site in real time. Many scientists from both CPC and EMC monitored different aspects of the reanalysis during this 2-year process. There were many times that the reanalysis was halted to address concerns that something may have gone wrong, and many corrections, backups, and restarts were made to ensure that the process was done as correctly and homogeneously as possible. An extremely large atlas of plots depicting nearly all aspects of the CFSR is available online at <http://cfs.ncep.noaa.gov/cfsr>.

A companion reanalysis for CFSR, called CFSR-Lite, is now in preparation at NCEP, which will reanalyze the global atmosphere at resolution T126L64, from 1948 through 2010. It will be conducted in only two streams with the break between 1978 and 1979, in order to reduce discontinuities, which were problematic at the five CFSR stream boundaries. It is anticipated to complete this project sometime in 2012.

A.4 JMA JRA-25

The Japan Meteorological Agency (JMA) and the Central Research Institute of Electric Power Industry conducted the Japanese 25-year re-analysis (JRA-25, Onogi et al., 2007) covering the period from 1979 to 2004. JRA-25 uses 3D-Var. The model has a spectral resolution of T106 (equivalent to a horizontal grid size of around 120 km) and 40 vertical layers with the top level at 0.4 hPa. Most of the observational data used in ERA-40 were used, however additional data such as wind profile retrievals surrounding tropical cyclones (TCRs) supplied by Dr. M. Fiorino and daily snow depth observations recorded in “Monthly Surface Meteorological Data in China”

published by CMA and digitized by MRI/JMA were also used. The reanalysis was conducted in two streams, one from 1979 to 1991, and one from 1991 to 2004. JRA-25 products (both six-hourly and monthly mean) are available from http://jra.kishou.go.jp/JRA-25/index_en.html.

A.5 JMA JRA-55

Since the workshop, JMA started their new atmospheric reanalysis, JRA-55 (Ebita et al., 2011), with plans to cover a 55-year period from 1958. The goal of JRA-55 is to provide a comprehensive atmospheric dataset suitable for studies of climate change or multi-decadal variability. The system uses an updated JMA operational NWP system, with a new radiation scheme to the forecast model and 4D-Var with Variational Bias Correction (VarBC) for satellite radiances. The model grid is TL319L60 (~60km) with a top layer at 0.1 hPa. A simple inflation factor (x 1.8) is applied to the background error covariances before 1972. The RAOBCORE v1.4 correction of Haimberger (2007) has been applied to the radiosondes. The system uses time-varying greenhouse gas concentrations and prescribed ozone and aerosol properties. The entire JRA-55 production is expected to be completed in early 2013. Thereafter, JRA-55 will be continued as a new JCDAS on real time basis.

A.6 NOAA-CIRES 20CR

The “20th Century Reanalysis Project” version 2 (20CR) has recently been generated by Compo et al. (2011). Led by NOAA and CIRES, the 20CR project is an international collaborative effort to produce a comprehensive global atmospheric circulation dataset spanning the twentieth century, assimilating only surface observations of synoptic pressure and using the UK Met Office HadISST (Rayner et al., 2003) monthly sea surface temperature and sea ice distributions as boundary conditions. Radiative forcings of time-varying solar output, volcanic aerosols, and CO₂ were also prescribed as in Saha et al. (2010).

20CR provides the first estimates of global tropospheric variability spanning 1871 to the present at 6-hourly temporal and 2° spatial resolutions. It uses, together with an experimental 2008 version of the global NWP model developed at NCEP to provide background “first guess” fields, a recently developed Ensemble Kalman Filter data assimilation method (Whitaker and Hamill, 2002). This directly yields a global analysis every 6 hours as the most likely state of the atmosphere, and also yields the uncertainty of that analysis. Earlier work established the feasibility of producing such a reanalysis dataset from the 1850s to present using only surface observations (Whitaker et al., 2004; Anderson et al., 2005; Compo et al., 2006; Whitaker et al., 2009).

20CR was processed in 27 approximately 5-year streams (see Compo et al., 2011 Table III). These data are available six-hourly at 2° horizontal resolution on 24 pressure levels from NOAA ESRL (<http://go.usa.gov/XTd>) and NCAR (<http://rda.ucar.edu/datasets/ds131.1>) and will also be distributed via the NOAA National Model Archive and Distribution System (NOMADS; <http://nomads.ncdc.noaa.gov>). Selected fields from individual ensemble members are also available via the NERSC Science Gateway (<http://portal.nersc.gov>). Additionally, the complete spectral files for every ensemble member were archived, so any additional variable can be obtained for every member. Finally, the results of the assimilation of each observation in the ISPD, including the first guess and analysis uncertainty at the observation location, are also available courtesy of NCAR (<http://rda.ucar.edu/datasets/ds132.0>).

Appendix B: Summary of Reanalyses to Date

Reanalysis	Organization	Time Span	Resolution	Method	Radiances	VarBC
GEOS-1	DAO	3/1985-11/1995	2×2.5×14L	OI	No	No
ERA-15	ECWMF	1979-1993	T106L31	OI	No	No
NCEP-NCAR R1	NCEP	1948-present	T62L28	3D-Var	No	No
NCEP-DOE R2	NCEP	1979-present	T62L28	3D-Var	No	No
NARR	NCEP	1979-present	32km	3D-Var	Yes	Yes
CFSR	NCEP	1979-present	T382L64	3D-Var	Yes	Yes
CFSR-Lite *	NCEP	1948-present	T126L64	Hybrid EnKF	Yes	Yes
ERA-40	ECMWF	9/1957-8/2002	T159L60	3D-Var	Yes	No
JRA-25	JMA	1979-2004	T106L40	3D-Var	Yes	No
ERA-Interim	ECMWF	1979-present	T255L60	4D-Var	Yes	Yes
MERRA	GMAO	1979-present	½ × 2/3 × 72L	3D-Var	Yes	Yes
JRA-55 *	JMA	1958-present	TL319L60	4D-Var	Yes	Yes
20CR	NOAA-CIRES	1871-2010	T62L28	EnKF	No	No

*not yet at real-time

Appendix C: Acronyms

20CR	(NOAA-CIRES) Twentieth Century Reanalysis
3D-Var	Three-dimensional Variational assimilation
4D-Var	Four-dimensional Variational assimilation
ACRE	Atmospheric Circulation Reconstructions over the Earth
AGCM	Atmospheric General Circulation Model
AIRS	Advanced Infra-Red Sounder
AMSU	Advanced Microwave Sounding Unit
CAMS	Climate Anomaly Monitoring System
CCSP	(U.S.) Climate Change Science Program
CDAS	Climate Data Assimilation System
CERES	Clouds and the Earth's Radiant Energy System
CFS	Climate Forecast System
CFSR	Climate Forecast System Reanalysis
CHAMP	Challenging Minisatellite Payload
CIRES	Cooperative Institute for Research in Environmental Sciences
CMA	Chinese Meteorological Administration
CMAP	CPC Merged Analysis of Precipitation
COSMIC	Constellation Observing System for Meteorology Ionosphere and Climate
CPC	(NOAA) Climate Prediction Center
CRIEPI	Central Research Institute of Electric Power Industry
DAO	Data Assimilation Office
DOE	Department of Energy
ECMWF	European Center for Medium-range Weather Forecasting
EnKF	Ensemble Kalman Filter Assimilation
EIG	Eastward Inertio-gravity wave
EMC	Environmental Modeling Center
ENSO	El Niño-Southern Oscillation
EOS	(NASA's) Earth Observing System
ER	Equatorial Rossby wave
ERS	European Remote Sensing Satellite
ESA	European Space Agency
ESRL	(NOAA) Earth System Research Laboratory
EUMETSAT	European Organisation for the Exploitation of Meteorological Satellites
GCOS	Global Climate Observing System
GEOS	Goddard Earth Observing System
GES DISC	Goddard Earth Sciences Data and Information Services Center
GFS	Global Forecast System
GHCN	Global Historical Climate Network
GMAO	Global Modeling and Assimilation Office
GMS	Geostationary Meteorological Satellite
GOME	Global Ozone Monitoring Experiment
GPCP	Global Precipitation Climatology Project
GSI	Gridpoint Statistical Interpolation
GSICS	Global Space-based Inter-Calibration System
IAU	Incremental Analysis Update
ISPD	International Surface Pressure Databank
JRA	Japanese Re-Analysis
JMA	Japan Meteorological Agency

KMA	Korea Meteorological Administration
MERRA	Modern Era Retrospective-analysis for Research and Applications
MJO	Madden-Julian Oscillation
MODIS	Moderate Resolution Imaging Spectroradiometer
MRG	Mixed Rossby-gravity wave
MSU	Microwave Sounding Unit (part of TOVS)
NARR	North American Regional Reanalysis
NASA	National Aeronautics and Space Administration
NCAR	National Centers for Atmospheric Research
NCAS	National Centre for Atmospheric Science
NCDC	National Climatic Data Center
NCEP	National Centers for Environmental Prediction
NCEP R1	NCEP-NCAR Reanalysis 1
NCEP R2	NCEP-DOE Reanalysis 2
NCO	NCEP Central Operations
NESDIS	National Environmental Satellite, Data, and Information Service
NOAA	National Oceanic and Atmospheric Administration
NOMADS	NOAA National Model Archive and Distribution System
NWP	Numerical Weather Prediction
OMI	Ozone Monitoring Instrument
QBO	Quasi-Biennial Oscillation
QC	Quality Control
R1	NCEP-NCAR Reanalysis 1
R2	NCEP-NCAR Reanalysis 2
RAOBCORE	Radiosonde Observation Correction using Reanalyses
RMS	Root Mean Square
SBUV	Solar Backscatter Ultraviolet Spectral Radiometer
SNO	Simultaneous Nadir Overpass
SSM/I	Special Sensor Microwave Imager
SSU	Stratospheric Sounding Unit
TCR	Tropical Cyclone
TRMM	Tropical Rainfall Measuring Mission
VarBC	Variational Bias Correction
WCRP	World Climate Research Program
WOAP	WCRP Observations and Analyses Panel

Appendix D: Acknowledgements

The GMAO gratefully acknowledges support from NASA's Modeling, Analysis, and Prediction program for the development and production of MERRA. Support from the NASA Center for Climate Simulation (NCCS) at Goddard Space Flight Center, in providing computational resources and a production environment for timely delivery of MERRA, was essential to the project. Support from the Goddard Earth Sciences Data and Information Services Center (GES DISC) for having MERRA distributed online is also greatly appreciated.

ECMWF reanalysis is the product of many years of outstanding scientific research and development by a large number of individuals at ECMWF and elsewhere. Human as well as technical resources for computing, data services, and user support at ECMWF are greatly appreciated. Preparation and production of ERA-Interim has been supported by staff secondments from the NCAS, the JMA, and the KMA.

NOAA/NCEP acknowledges the NOAA Climate Program Office (reanalysis grant) for funding part of CFSR. Contributions from the staff of EMC, CPC, NCEP Central Operations (NCO), and NESDIS are also gratefully acknowledged.

JRA-25 was operated as a joint research project between JMA and CRIEPI and was supported by many staff and research scientists. CRIEPI's Fujitsu VP5000 was the primary supercomputer used for JRA-25 production.

The JRA-55 project has been supported by a large number of the JMA staff members in many aspects including planning of the project, preparation of observational data, testing the data assimilation system, production and verification. Their support is greatly appreciated.

20CR gratefully acknowledges support provided by the US Department of Energy, Office of Science Innovative and Novel Computational Impact on Theory and Experiment (DOE INCITE) program, and Office of Biological and Environmental Research (BER), and by the NOAA Climate Goal. The project used resources of the National Energy Research Scientific Computing Center and of the National Center for Computational Sciences at Oak Ridge National Laboratory.

International collaborations with data providers from many institutions have been invaluable and essential to all the reanalyses and are gratefully acknowledged.

Previous Volumes in This Series

- Volume 1**
September 1994
Documentation of the Goddard Earth Observing System (GEOS) general circulation model - Version 1
L.L. Takacs, A. Molod, and T. Wang
- Volume 2**
October 1994
Direct solution of the implicit formulation of fourth order horizontal diffusion for gridpoint models on the sphere
Y. Li, S. Moorthi, and J.R. Bates
- Volume 3**
December 1994
An efficient thermal infrared radiation parameterization for use in general circulation models
M.-D. Chou and M.J. Suarez
- Volume 4**
January 1995
Documentation of the Goddard Earth Observing System (GEOS) Data Assimilation System - Version 1
James Pfaendtner, Stephen Bloom, David Lamich, Michael Seablom, Meta Sienkiewicz, James Stobie, and Arlindo da Silva
- Volume 5**
April 1995
Documentation of the Aries-GEOS dynamical core: Version 2
Max J. Suarez and Lawrence L. Takacs
- Volume 6**
April 1995
A Multiyear Assimilation with the GEOS-1 System: Overview and Results
Siegfried Schubert, Chung-Kyu Park, Chung-Yu Wu, Wayne Higgins, Yelena Kondratyeva, Andrea Molod, Lawrence Takacs, Michael Seablom, and Richard Rood
- Volume 7**
September 1995
Proceedings of the Workshop on the GEOS-1 Five-Year Assimilation
Siegfried D. Schubert and Richard B. Rood
- Volume 8**
March 1996
Documentation of the Tangent Linear Model and Its Adjoint of the Adiabatic Version of the NASA GEOS-1 C-Grid GCM: Version 5.2
Weiyu Yang and I. Michael Navon
- Volume 9**
March 1996
Energy and Water Balance Calculations in the Mosaic LSM
Randal D. Koster and Max J. Suarez
- Volume 10**
April 1996
Dynamical Aspects of Climate Simulations Using the GEOS General Circulation Model
Lawrence L. Takacs and Max J. Suarez
- Volume 11**
May 1997
Documentation of the Tangent Linear and its Adjoint Models of the Relaxed Arakawa-Schubert Moisture Parameterization Package of the NASA GEOS-1 GCM (Version 5.2)
Weiyu Yang, I. Michael Navon, and Ricardo Todling
- Volume 12**
August 1997
Comparison of Satellite Global Rainfall Algorithms
Alfred T.C. Chang and Long S. Chiu
- Volume 13**
December 1997
Interannual Variability and Potential Predictability in Reanalysis Products
Wie Ming and Siegfried D. Schubert

- Volume 14**
August 1998 A Comparison of GEOS Assimilated Data with FIFE Observations
Michael G. Bosilovich and Siegfried D. Schubert
- Volume 15**
June 1999 A Solar Radiation Parameterization for Atmospheric Studies
Ming-Dah Chou and Max J. Suarez
- Volume 16**
November 1999 Filtering Techniques on a Stretched Grid General Circulation Model
Lawrence Takacs, William Sawyer, Max J. Suarez, and Michael S. Fox-Rabinowitz
- Volume 17**
July 2000 Atlas of Seasonal Means Simulated by the NSIPP-1 Atmospheric GCM
Julio T. Bacmeister, Philip J. Pegion, Siegfried D. Schubert, and Max J. Suarez
- Volume 18**
December 2000 An Assessment of the Predictability of Northern Winter Seasonal Means with the NSIPP1 AGCM
Philip J. Pegion, Siegfried D. Schubert, and Max J. Suarez
- Volume 19**
July 2001 A Thermal Infrared Radiation Parameterization for Atmospheric Studies
Ming-Dah Chou, Max J. Suarez, Xin-Zhong, and Michael M.-H. Yan
- Volume 20**
August 2001 The Climate of the FVCCM-3 Model
Yehui Chang, Siegfried D. Schubert, Shian-Jiann Lin, Sharon Nebuda, and Bo-Wen Shen
- Volume 21**
September 2001 Design and Implementation of a Parallel Multivariate Ensemble Kalman Filter for the Poseidon Ocean General Circulation Model
Christian L. Keppenne and Michele M. Rienecker
- Volume 22**
August 2002 Coupled Ocean-Atmosphere Radiative Model for Global Ocean Biogeochemical Models
Watson W. Gregg
- Volume 23**
November 2002 Prospects for Improved Forecasts of Weather and Short-term Climate Variability on Subseasonal (2-Week to 2-Month) Time Scales
Siegfried D. Schubert, Randall Dole, Huang van den Dool, Max J. Suarez, and Duane Waliser
- Volume 24**
July 2003 Temperature Data Assimilation with Salinity Corrections: Validation for the NSIPP Ocean Data Assimilation System in the Tropical Pacific Ocean, 1993–1998
Alberto Troccoli, Michele M. Rienecker, Christian L. Keppenne, and Gregory C. Johnson
- Volume 25**
December 2003 Modeling, Simulation, and Forecasting of Subseasonal Variability
Duane Waliser, Siegfried D. Schubert, Arun Kumar, Klaus Weickmann, and Randall Dole
- Volume 26**
April 2005 Documentation and Validation of the Goddard Earth Observing System (GEOS) Data Assimilation System – Version 4
Senior Authors: S. Bloom, A. da Silva and D. Dee

Contributing Authors: M. Bosilovich, J-D. Chern, S. Pawson, S. Schubert, M. Sienkiewicz, I. Stajner, W-W. Tan, and M-L. Wu

Volume 27
December 2008

The GEOS-5 Data Assimilation System - Documentation of Versions 5.0.1, 5.1.0, and 5.2.0.

M.M. Rienecker, M.J. Suarez, R. Todling, J. Bacmeister, L. Takacs, H.-C. Liu, W. Gu, M. Sienkiewicz, R.D. Koster, R. Gelaro, I. Stajner, and J.E. Nielsen

Volume 28
April 2012

The GEOS-5 Atmospheric General Circulation Model: Mean Climate and Development from MERRA to Fortuna

Andrea Molod, Lawrence Takacs, Max Suarez, Julio Bacmeister, In-Sun Song, and Andrew Eichmann

REPORT DOCUMENTATION PAGE

*Form Approved
OMB No. 0704-0188*

The public reporting burden for this collection of information is estimated to average 1 hour per response, including the time for reviewing instructions, searching existing data sources, gathering and maintaining the data needed, and completing and reviewing the collection of information. Send comments regarding this burden estimate or any other aspect of this collection of information, including suggestions for reducing this burden, to Department of Defense, Washington Headquarters Services, Directorate for Information Operations and Reports (0704-0188), 1215 Jefferson Davis Highway, Suite 1204, Arlington, VA 22202-4302. Respondents should be aware that notwithstanding any other provision of law, no person shall be subject to any penalty for failing to comply with a collection of information if it does not display a currently valid OMB control number.

PLEASE DO NOT RETURN YOUR FORM TO THE ABOVE ADDRESS.

1. REPORT DATE (DD-MM-YYYY) 30-06-2012		2. REPORT TYPE Technical Memorandum		3. DATES COVERED (From - To)	
4. TITLE AND SUBTITLE Technical Report Series on Global Modeling and Data Assimilation, Volume 29; Atmospheric Reanalyses—Recent Progress and Prospects for the Future. A Report from a Technical Workshop, April 2010				5a. CONTRACT NUMBER	
				5b. GRANT NUMBER	
				5c. PROGRAM ELEMENT NUMBER	
6. AUTHOR(S) Max J. Suarez, Editor Michele M. Rienecker, Dick Dee, Jack Woollen, Gilbert P. Compo, Kazutoshi Onogi, Ron Gelaro, Michael G. Bosilovich, Arlindo da Silva, Steven Pawson, Siegfried Schubert, Max Suarez, Dale Barker, Hirotaka Kamahori, Robert Kistler, and Suranjana Saha				5d. PROJECT NUMBER	
				5e. TASK NUMBER	
				5f. WORK UNIT NUMBER	
7. PERFORMING ORGANIZATION NAME(S) AND ADDRESS(ES) NASA, Goddard Space Flight Center Greenbelt, MD 20771				8. PERFORMING ORGANIZATION REPORT NUMBER	
9. SPONSORING/MONITORING AGENCY NAME(S) AND ADDRESS(ES) National Aeronautics and Space Administration Washington, DC 20546-0001				10. SPONSORING/MONITOR'S ACRONYM(S) NASA GSFC	
				11. SPONSORING/MONITORING REPORT NUMBER TM-2012-104606/Vol29	
12. DISTRIBUTION/AVAILABILITY STATEMENT Unclassified-Unlimited, Subject Category: 47 Report available from the NASA Center for Aerospace Information, 7115 Standard Drive, Hanover, MD 21076. (443)757-5802					
13. SUPPLEMENTARY NOTES					
14. ABSTRACT In April 2010, developers representing each of the major reanalysis centers met at Goddard Space Flight Center to discuss technical issues – system advances and lessons learned – associated with recent and ongoing atmospheric reanalyses and plans for the future. The meeting included overviews of each center’s development efforts, a discussion of the issues in observations, models and data assimilation, and, finally, identification of priorities for future directions and potential areas of collaboration. This report summarizes the deliberations and recommendations from the meeting as well as some advances since the workshop.					
15. SUBJECT TERMS Meteorology, Climatology, Modeling					
16. SECURITY CLASSIFICATION OF:			17. LIMITATION OF ABSTRACT Unclassified	18. NUMBER OF PAGES 56	19a. NAME OF RESPONSIBLE PERSON Max Suarez
a. REPORT Unclassified	b. ABSTRACT Unclassified	c. THIS PAGE Unclassified			19b. TELEPHONE NUMBER (Include area code) (301) 614-5292

